8-1-2012

Interactions Among Evaporation, Ice Cover, and Water Temperature on Lake Superior: Decadal, Interannual, and Seasonal Variability

Katherine Van Cleave
University of Nebraska-Lincoln, vancleave.katie@gmail.com

INTERACTIONS AMONG EVAPORATION, ICE COVER, AND WATER TEMPERATURE ON LAKE SUPERIOR: DECADAL, INTERANNUAL, AND SEASONAL VARIABILITY

by
Katherine Van Cleave

A THESIS

Presented to the Faculty of
The Graduate College at the University of Nebraska
In Partial Fulfillment of Requirements
For the Degree of Master of Science

Major: Natural Resource Sciences

Under the Supervision of Professor John D. Lenters

Lincoln, Nebraska

August, 2012

INTERACTIONS AMONG EVAPORATION, ICE COVER, AND WATER TEMPERATURE ON LAKE SUPERIOR: DECADAL, INTERANNUAL, AND SEASONAL VARIABILITY

Katherine Van Cleave, M.S.

University of Nebraska, 2012

Adviser: John D. Lenters

Lake Superior, the largest freshwater lake in the world by surface area, has enormous impacts on the regional weather and climate. The lake also comprises over half of the total water volume in the Great Lakes system and is an important resource for commercial shipping, water supplies, hydropower, recreation, and aquatic ecosystems. Water temperature and evaporation on Lake Superior have been found to be increasing in recent decades, while ice cover has been decreasing at a very rapid pace. A careful analysis of the long-term trends, however, shows that these changes have not been linear through time. Rather, a step-change occurred in 1997/98 that resulted in a drop in ice duration of nearly 40 days, a 3°C increase in summer water temperature, and a near doubling of July-August evaporation rates. Linear regression analysis of data on either side of this step change shows trends which are largely insignificant and even opposite in sign from those of the step change. Using time-lagged correlation and composite analysis, interactions among ice cover, water temperature, and evaporation are explored across seasonal and interannual timescales. Fall evaporation rates are found to be significantly correlated with ice cover in the following winter, presumably as a result of strong latent heat flux leading to rapid ice onset and growth. Similarly, ice cover is found to be a strong determinant of summer water temperature. This, in turn, can lead to changes in late-summer evaporation rates. Quantifying these complex interactions is important for assessing the potential impacts of future climate change on large-lake systems. Key to this understanding is the direct measurement of lake surface processes such as evaporation and sensible heat flux. As such, this study includes an analysis of the first direct observations of nearshore evaporation rates on the Great Lakes, using eddy covariance data collected from a monitoring station on Granite Island (near Marquette, Michigan). The data are analyzed for the period October 2010 to April 2012 to explore the seasonal and interannual variations in latent and sensible heat fluxes over Lake Superior, as well as some of the primary climatic factors driving this variability.

Acknowledgements

I would like to thank firstly those who served as my graduate committee in the completion of this thesis: John Lenters, Andy Suyker, and Diego Riveros-Iregui, as well as those who contributed additional advice in the studies presented, specifically Chris Spence, Peter Blanken, and Jia Wang.

Water temperature, evaporation, and ice cover data for this study were obtained from the Great Lakes Environmental Research Laboratory (GLERL), with help especially from Ray Assel, Anne Clites, and Tim Hunter. Additional water temperature data were retrieved from the National Buoy Data Center (NDBC). A special thanks to Dan Hatch at the University of Nebraska-Lincoln (UNL) and James Kathilankal at LI-COR for helping with the eddy covariance data processing.

The station and data from Granite Island would not have been possible without the assistance of Scott Holman (landowner), Mike Smith, and Dan "Ducky," who helped maintain the island power supplies, internet, and other infrastructure. Also, I would like to thank Tracy Twine at the University of Minnesota for the use of the LI-7500 instrument. Many colleagues and friends have assisted with fieldwork at Granite Island, including Ben Scheelk, Brittany Potter, and Srikanth Kondabalu, and I thank them for braving the waves to help keep the station running.

Finally, this thesis would not have been possible without generous funding from the UNL School of Natural Resources, UNL Chancellor's Fellowship, William J. Curtis Fellowship, UNL Water Resources Research Initiative, and the Great Lakes Integrated Sciences and Assessments (GLISA) Center. In addition, I would like to acknowledge the Larrick-Whitmore Student Travel Grant for assisting with travel

support to the International Association for Great Lakes Research (IAGLR) Annual Conference in Duluth, Minnesota (June 2011), where a portion of this research was presented.

Table of Contents

List of Tables and Figures

CHAPTER 1: INTRODUCTION

1. Background

Lake Superior, the largest freshwater lake by surface area (82,103 km^2) in the world, has an effect that reaches far beyond its regional climate. Water from Lake Superior, or the Ojibwe name *Gichigami* (meaning "big water") flows through the Soo Locks in Sault Ste. Marie, onwards to the other four Laurentian Great Lakes, and eventually to the Atlantic Ocean through the St. Lawerence Seaway. Changes in this enormous body of water can have far-reaching physical, ecological, and anthropogenic effects.

Many notable changes in the lake have already been documented. Summer water temperatures over the lake have been found to be increasing faster than the ambient air temperature (Lenters 2004); (Austin and Colman 2007). During the past few dacades, Lake Superior has also experienced a 79% decrease in ice cover (Assel 2003); (Wang 2011). It has been suggested, in fact, that the reductions in Lake Superior ice cover are mechanistically related to the increases in summer water temperature [i.e., through ice-albedo feedbacks and the timing and duration of the summer stratification period; (Austin and Colman 2007). Further connections to summer evaporation rates and changes in lake level are also likely, as evidenced by recent increases in summer evaporation that have been noted for Lake Michigan-Huron (Hanrahan 2010) and smaller, inland lakes in the Great Lakes region (Mishra 2010).

This study aims to quantify, analyze, and compare the changes in the interacting variables of summer water temperature, evaporation, and ice cover on

Lake Superior. The first chapter will address the long-term trends in these variables, both linear and non-linear. Following that, chapter 2 will present correlation and composite analyses in order to determine connections and relationships among the same variables from seasonal to interannual timescales. The third chapter of this study will present data from an eddy covariance station on Granite Island, Michigan (located roughly 20 km north of Marquette, Michigan). Interannual and seasonal patterns will be analyzed, and the results are then compared to an offshore station located at Stannard Rock Light (located on a shoal 55 km northeast of Granite Island).

2. Research Questions

This study will address the following questions:

1) What are the long-term trends (linear and non-linear) in evaporation, water temperature, and ice cover on Lake Superior over the historical record (1979-2010)?
2) How do evaporation, water temperature, and ice cover co-vary and interact with each other to influence interannual and seasonal variability of evaporation, water temperature, and ice cover?
3) What is the seasonal variability in evaporation rates and associated surface energy balance in the nearshore regions of Lake Superior (as measured at Granite Island)?
4) What are the climatic and limnological controls on this variability (wind, temperature, humidity, ice cover), and how do they help to explain the interactions among evaporation, water temperature, and ice cover?

CHAPTER 2: LONG-TERM CHANGES IN LAKE SUPERIOR ICE COVER, EVAPORATION, AND SUMMER WATER TEMPERATURE: A REGIME SHIFT IN 1997/98

1. Introduction

Increases in lake surface temperature have been widely documented in recent years throughout North America (Anderson 1996, McCormick and Fahnenstiel 1999, Schneider 2009), as well as globally (Schneider and Hook 2010). This warming is especially apparent for the Laurentian Great Lakes, where summer water temperatures are generally found to be increasing faster than the ambient air temperature, particularly for Lake Superior (Lenters 2004, Austin and Colman 2007). During approximately the same time period, lake ice duration has been decreasing in many regions of the world (Hanson 1992, Robertson 1992, Assel and Robertson 1995, Magnuson 2000, Hodgkins 2002, Futter 2003, Duguay 2006, Jensen 2007). Again, this is especially true for Lake Superior, which has experienced a 79% decrease in ice cover over the past few decades (Assel 2003); (Wang 2011). It has been suggested, in fact, that the reductions in Lake Superior ice cover are mechanistically related to the concomitant increases in summer water temperature [i.e., through ice-albedo feedbacks and the timing and duration of the summer stratification period; (Austin and Colman 2007). Further connections to summer evaporation rates and changes in lake level are also likely, as evidenced by recent increases in summer evaporation that have been noted for Lake Michigan-Huron (Hanrahan 2010) and smaller, inland lakes in the Great Lakes region (Mishra 2010).

Most of the previous studies noted above have used standard linear regression techniques to assess rates of change. This is often an appropriate method

for many lake systems that undergo relatively linear changes through time. However, as we show in the current study, this turns out not to be the case for Lake Superior. Instead, the majority of the long-term "trend" in each of the prominent trending variables (ice cover, water temperature, and evaporation) is associated with a pronounced, non-linear "regime shift" that occurred around 1997/98. In the following sections, we examine the data and methodology used to assess changes in the different lake variables, as well as a discussion of the mean seasonal variability in Lake Superior water temperature, ice cover, and evaporation. After a description of the step-change analysis that is used to detect the timing of the regime shift, we then present an analysis of the long-term trends and non-linear shifts in each of these variables. Finally, we conclude by summarizing the overall results, examining potential large-scale mechanisms for the observed regime shift, and discussing the broader implications of the work.

2. Data and Methodology

2.1. Water Temperature and Evaporation

Hourly water temperature data were obtained from three National Data Buoy Center (NDBC) buoys located in the offshore regions of Lake Superior (Eastern, 45004; Central, 45001; and Western, 45006). These buoys are deployed each year after ice melt, but before the beginning of the stratified season (typically by late April or early May). They are removed from the lake by late October or early November (i.e., before ice-onset). Data gaps are generally short, with the exception of the western buoy during 2007, for which no data were available. The buoys measure the "bulk" water temperature at a depth of 60-100 cm and have initial

deployment dates of 1979 (central), 1980 (eastern), and 1981 (western). For the purposes of this study, we examine the full period of record from 1979-2010 using an aggregation of the three NDBC buoys (described in the next paragraph).

Basic quality control checks were performed to identify any major outliers in the hourly water temperature data, and steps were taken to properly fill data gaps prior to creating monthly averages. For example, linear interpolation was used to fill any data gaps that were less than or equal to six hours in length, with gaps of seven hours or longer left as "missing." The hourly values were then averaged to daily means, and days that were missing more than 25% of the hourly values (i.e., total of 7 hours or longer) were left as missing. The daily mean data were then interpolated and averaged to monthly means through a similar process (i.e., applied only to months that had fewer than 8 days of missing data). Finally, any remaining missing data in the monthly means were filled through regressions with monthly mean data from the most representative adjacent buoy (for a given month, and across all years), and all three buoys were then averaged together to create a monthly timeseries of "mean offshore" water temperature. A few remaining months during which all three buoys had missing data were filled with regressions against adjacent monthly means (e.g., June vs. July). The end result is a complete record of monthly offshore surface water temperature for the period May-October, 1979-2010.

In addition to the in situ buoy records, model estimates of "lake-wide mean" surface water temperature and evaporation were obtained for 1948-2009 from the National Oceanic and Atmospheric Administration (NOAA) Great Lakes Environmental Research Laboratory [GLERL; (Hunter and Croley 1993). Provisional

estimates of 2010 water temperature and evaporation were also provided by GLERL (T. Hunter, personal communication; 1 February 2011). This 1948-2010 dataset provides daily estimates of surface water temperature and evaporation rate using a 1-D thermodynamic model (Croley 1989, Croley and Assel 1994) forced by meteorological observations (mostly nearshore, but extrapolated and adjusted to provide over-lake estimates). The model output is available year-round, as opposed to the NDBC buoy data, which is only available during the ice-free season. Similar to the NDBC water temperature data, the GLERL model output was also averaged from daily to monthly values to provide a complete record of monthly mean lake-wide surface water temperature and evaporation rates for the period 1979-2010.

For the purposes of the trend analysis, and to be consistent with previous studies [e.g., (Austin and Colman 2007)], we also created 3-month summer-mean water temperatures based on the period July-September (JAS), both for the buoy data and the GLERL model output. We generally found very good agreement between the NDBC and GLERL datasets, in terms of the interannual variability and long-term trends. The NDBC JAS water temperatures tend to be ~3°C cooler than the GLERL estimates, on average. But this is to be expected, given that the buoys are deployed well offshore, while the GLERL model represents a bulk estimate for the entire lake (i.e., including nearshore regions). Mean summer evaporation rates were calculated for the 2-month period July-August (JA), since these were the only two months in the GLERL model output that exhibited significant trends in lake evaporation during the study period (1979-2010). This is similar to Lenters (2004),

who found significant upward trends in Lake Superior evaporation for the months of June, July, August, and October (for the period 1948-1999).

2.2. Ice Cover Data and Derived Metrics

Ice cover records for Lake Superior were obtained from the NOAA Great Lakes Ice Atlas for the period 1973-2002 (available from http://www.glerl.noaa.gov/data/ice/atlas), with supplementary data for 2003-2005 provided by (Assel 2005). The data consist of composite ice charts and a blend of observations from various sources covering the Great Lakes region (ships, aircraft, satellites, and shore-based observations). Additional data for the period 2006-2010 were obtained from researchers at NOAA GLERL (A. Clites, personal communication; 2 March 2011). The ice cover records in each dataset provide the fraction of the total lake surface area, f, that is covered by ice. The raw observations are available on a roughly bi-weekly basis from early December through late April or May and were linearly interpolated to obtain a daily timeseries for the entire 38-year period (1973-2010). 15-day running means were then calculated in order to provide a smoother, robust timeseries for examining ice cover timing (onset, duration, etc.).

The 15-day running mean fractional ice coverage, f_{15}, was used to derive a number of different ice metrics for this study. First, we define the "ice-on date" to be the day on which f_{15} first reaches 0.05 (i.e., ≥5% ice coverage). Similarly, "ice-off" is defined as the last day of ice coverage that is ≥5%, and ice "duration" is the length of time between ice-on and ice-off. The 5% threshold was chosen based on an examination of the distribution of "first ice" values in the raw dataset, as well as the

maximum f_{15} value reached during each of the 38 winters. Two years, for example, reached a maximum f_{15} of only ~0.08 (1997/98 and 2001/02). For the occasional years in which f_{15} started or ended above 0.05, linear extrapolation was used to identify the 5% ice-on or ice-off date. (This was required for 12 of the 38 ice-on dates and 7 of the 38 ice-off dates, for an average extrapolation length of only 7.7 days.) It should also be noted that – although it is possible for ice coverage to rise and fall above the 5% threshold multiple times within a given winter – the 15-day smoothing process minimizes the likelihood of such events, causing it to occur only once during the entire 38-year period (an 8-day interval in the winter of 1998/99). Therefore, we ignore this one event and consider total "ice duration" to simply be the period from ice-on to ice-off.

In addition to the 5% ice-on / ice-off dates and total ice duration, we also calculated the winter-mean ice coverage for each year (based on the average of all f_{15} values from ice-on to ice-off). The maximum winter ice coverage (i.e., maximum f_{15} value) and the date on which it occurred were also determined for each year. The final ice metric that was calculated is something that we refer to as "ice fraction days," or IFD (similar, for example, to the concept of freezing degree days). Here, IFD is simply defined as the cumulative ice fractional area from ice-on to ice-off (i.e., IFD = $\sum(f_{15} \cdot \Delta t)$, where Δt is one day, and the summation period is limited to the overall 5% ice-on/ice-off interval, when $f_{15} \geq 0.05$). Note that IFD is equal to the product of the mean fractional ice coverage and total ice duration and is, therefore, a useful integrative measure of overall "winter severity." An IFD of 30 days, for example, would be equivalent to 30 days of 100% ice coverage (or 60 days of 50% coverage,

etc.). In total, seven different ice metrics for Lake Superior were examined in this study for the period 1973-2010.

2.3. Step-change and Linear Trend Analyses

In order to identify decadal-scale step changes within the dataset, a 20-year moving window (split into two 10-year periods) was propagated through the time series, calculating means for both the first and second 10-year periods. A Mann-Whitney U-test was then used to calculate the probability that the difference between these two means was statistically significant. This technique, therefore, identifies decadal "regime shifts" that occur within 20-year moving windows. Although longer averaging periods might be considered more desirable, the analysis is also constrained by the limited observational period of some of the datasets (e.g., 32 years, in the case of the NDBC water temperature). Thus, it was deemed that a two-decade moving window was suitable for the current study. For comparison purposes, we also calculated linear trends for each of the various timeseries using standard linear regression. The Mann-Kendall test was then applied to determine statistical significance.

3. Results

3.1. Mean Annual Cycle (1979-2010)

On average, Lake Superior shows a regular, seasonal progression in surface water temperature, evaporation, and ice cover (Figure 1). Monthly mean water temperatures typically peak in August, followed by a rapid decline in the autumn, as latent and sensible heat fluxes begin to increase. Monthly evaporation peaks in

December, which also coincides with the average onset of ice cover. Evaporation rates then begin to decline as water temperatures drop and ice cover increases (Figure 1). Although maximum ice cover and minimum water temperatures both typically occur in February and March, evaporation rates do not minimize until June, due to significant lags between water and air temperature and associated vapor pressure gradients (Lenters 2004). In summary, the connections among Lake Superior water temperature, evaporation, and ice cover are readily evident in the 3-4 month lags that exist within the mean annual cycle. Increases in evaporation contribute both to the decline in water temperature and to the onset of ice cover. Similarly, loss of ice cover and low evaporative cooling in spring both play a role in the rapid warming of surface water temperatures from April to August (in addition to the strong role of solar radiative heating). Besides the seasonal cycle presented here, it should also be noted that Lake Superior exhibits relatively strong interannual variability in temperature, evaporation, and ice cover. Summer (JAS) water temperatures, for example, can vary from 7 to 17°C on a year-to-year basis. Similarly, ice cover duration can vary by weeks to months, sometimes lasting from November to May, and other years lasting for only a few weeks in January.

3.2. Step-change Analysis

Results of the step-change analysis are illustrated in Figure 2 and Table 1 for the available period of Great Lakes ice cover records (1973-2010), showing examples for summer water temperature (Figure 2a), JA evaporation (Figure 2b), and winter IFD (Figure 2b). Step-change analysis of other ice cover metrics (duration, extent, etc.) shows similar results, and p-values for all parameters are

listed in Table 1. (Note that decadal shifts for the NDBC buoy data are not shown prior to 1989, since the dataset begins in 1979.) Figure 2 shows the differences in two, adjacent 10-year means, with the date on the x-axis showing the midpoint of the 20-year moving window (specifically, the year that starts the second decade). JAS surface water temperature shows statistically significant step changes in 1997, 1998, 1999, and 2000, both for the NDBC buoy observations and the GLERL model results (Figure 2a). A small step change is also evident in 1983 (for the GLERL data only), but with weaker statistical significance. 1998 shows the largest step change of all years, with summer water temperatures for the period 1998-2007 being roughly 2.5-3°C warmer than for the period 1988-1997 (a difference which is significant well beyond the 99% level; Table 1).

Similar step changes were found for evaporation and ice cover (Figure 2b), with both JA evaporation and winter IFD showing the largest decadal increase during 1998 (i.e., 1998-2007 compared to 1988-1997). For the purposes of this study, we refer to the winter "year" as being the latter portion of the winter season (e.g., 1998 refers to the winter of 1997/98). Examination of five of the remaining six ice cover metrics (ice-on, ice-off, duration, mean ice extent, and maximum ice extent; Table 1) all showed the largest, significant decadal changes during 1998. Only one ice metric (date of maximum ice extent) showed the largest significant step change to occur during a year other than 1998 (in this case, 1988). JA evaporation also shows evidence of a step change around 1983-1986 (Figure 2b), but only at the 95% significance level, and with no correspondingly significant shift in IFD. It is striking, however, to note the strong anticorrelation between decadal changes in winter IFD

and the following summer's JA evaporation (and JAS water temperature), suggesting that long-term changes in ice cover may be a useful predictor of summer conditions on the Great Lakes.

Due to the prevalence, magnitude, and strong statistical significance of the 1998 step change throughout six of the seven ice cover metrics, two independent summer water temperature estimates, and JA evaporation rates, we hereafter refer to this step change as the 1998 "regime shift" in Lake Superior. Weaker step changes (and in fewer parameters), such as during 1983 or 1988, are not considered in the current study. Consequently, we use 1998 as the break point at which to calculate mean values before and after the change. So, for example, when examining linear trends in ice cover duration for the period 1973-2010, we also calculate mean values for 1973-1997 and 1998-2010 to illustrate the regime shift that occurred in 1998. Although we are now comparing two periods of differing length (e.g., 25 years and 13 years), it is important to note that the timing of the shift was identified using a consistent, decadal interval. Furthermore, the differences in the means of the new, varying time periods remains statistically significant in all cases (at the 99% level).

3.3. Long-term Trends

Figure 3 shows the winter values and long-term trends in Lake Superior fractional ice coverage (Figure 3a) and IFD (Figure 3b), calculated using both standard linear regression and the 1998 step change analysis. Clearly, the lake has experienced a significant decline in ice cover over the past few decades, as has been noted in previous studies [e.g. (Wang 2011)]. This includes strong changes in 5% ice-on / ice-off dates and ice duration (Figure 3a), as well as a decline in IFD of ~8

days/decade (Figure 3b). There has also been a reduction in the frequency of years with high fractional ice coverage during the period 1973-2010 (e.g., years with ice coverage of 40% or more; Figure 3a). Interestingly, however, the changes illustrated in Figure 3 are anything but linear. Rather, when the linear trends are split into two time periods (at the 1998 break point), the long-term trends largely disappear or even reverse (e.g., in the case of ice-off date and IFD). In fact, none of the pre- or post-1998 linear trends in ice cover are statistically significant at the 90% level except for winter-mean ice extent, which actually shows an *increase* in ice extent after 1998 (at a rate of ~11% per decade). Together with the step changes illustrated in Figure 2, this demonstrates quite clearly that long-term changes in Lake Superior ice cover are not well represented by a simple, linear trend from 1973-2010. Rather, it is more appropriate to characterize the change as being associated with the aforementioned 1998 regime shift. In comparing the mean values of the ice cover metrics before and after 1998 (Figures 3 and 4), we find that both the 5% ice-on and ice-off dates have changed by almost 3 weeks (i.e., 19 days later and earlier, respectively), resulting in a 39-day reduction in ice duration. Similarly, IFD experienced a decline of 24 days in conjunction with the 1998 regime shift (i.e., 41 days to 17 days; Figure 3b). This reflects not only the reduction in 5% ice duration from 113 to 74 days, but also a decline in mean ice fraction from 34% to 19% (significant at the 99% level; Table 1). Maximum winter ice extent dropped from a mean value of 69% to 36% after 1998.

Analysis of the long-term trends in summer water temperature and evaporation rate (Figure 5) shows results similar to those already discussed for ice

cover. Namely, the JAS surface water temperature (both NDBC and GLERL) and JA evaporation show significant, linear increases through time (1979-2010; Figure 5a) that largely disappear when the 1998 break point is applied (Figure 5b). In one example (GLERL JAS water temperature), the linear trend after 1998 is actually significantly downward (-1.1 °C/decade; p=0.1), indicating lake *cooling* following the 1998 warming event. This is corroborated by the NDBC buoy data, which show an even larger rate of cooling (-1.5 °C/decade), although the statistical significance is weaker due to larger interannual variability. Similarly, JA evaporation shows a downward, but insignificant trend after 1998. Given these observations (and those in Figure 2), the average JAS water temperature and JA evaporation rates were calculated for the pre- and post-1998 periods to assess the magnitude of the regime shift (Figure 5c). The results show a step-change increase in summer water temperatures of ~2°C (GLERL) to 2.7°C (NDBC) following the 1998 event, as well as a near doubling of total JA evaporation (2.2 cm to 4.2 cm). All three step changes are statistically significant at the 99% level.

4. Discussion and Conclusions

The analysis presented here has uncovered two statistically distinct climatic regimes for Lake Superior, defined not only by ice cover, but also by summer water temperature and evaporation rate. Namely, the lake experienced a pronounced change during the winter of 1997/98, when ice cover reached (at that time) record-low values of mean/max ice fraction, IFD, and duration (Figure 3 and 4). This was followed by record-warm summer water temperatures (Figure 5) and near-record JA evaporation rates (surpassed only by 1987). There is some evidence that the lake

"recovered" somewhat from the anomalous 1997/98 event, showing later ice-off dates and greater winter-mean ice extent in subsequent years (Figure 3a), as well as increased IFD (Figure 3b), cooler summer water temperatures (Figure 5b), and reduced JA evaporation (Figure 5b). Most of these recovery trends are not, however, statistically significant, suggesting that the 1998 regime shift has largely been sustained. Furthermore, at the time of this writing, Lake Superior experienced a record-low ice year in 2011/12, eclipsing even the previous records set in 1997/98. Thus, it is likely that any recovery evident in Figures 3 and 4 has been significantly curtailed since 2010, or perhaps even eliminated.

It is notable that the 1998 regime shift in Lake Superior occurred at the same time as an anomalous climatic event (i.e., the warm El Niño winter of 1997/98). Although this does not imply that the entire, prolonged regime shift is causally linked to a single El Niño event, we did examine a number of teleconnection indices to assess their potential role. While the El Niño-Southern Oscillation (ENSO) pattern has a strong effect on winter temperatures and ice severity in the Great Lakes region (Assel 1998, Rodionov and Assel 2003), long-term variations in the Nino 3.4 index over the last few decades (not shown) do not readily explain the regime shift seen in 1997/98. In fact, in recent years, the negative phase of ENSO (i.e., La Niña) has dominated, which – by itself – would not be consistent with the warmer winters experienced over Lake Superior since 1997/98. Similarly, during this more recent period, the Arctic Oscillation (AO) has been split almost equally between cold and warm phases, suggesting that the AO is also not directly associated with the regime shift.

Warm phases of the Pacific Decadal Oscillation (PDO), in the absence of strong El Niño events, are coincident with more northerly flow over North America and, therefore, colder temperatures and greater ice cover over the Great Lakes (Rodionov and Assel 2003). The PDO has also been found to be temporally coherent with Lake Superior water levels, air temperature, and evaporation on interdecadal timescales (Ghanbari and Bravo 2008). Furthermore, a study of Lake Mendota (Wisconsin, USA), located southwest of Lake Superior, found the PDO to be temporally coherent with both ice duration and ice-off dates on interannual and interdecadal timescales (Ghanbari 2009). Beginning in 1977, a warm phase of the PDO began, coinciding with a significant, upward change in the PDO index (Figure 6). This warm phase persisted until 1998, when the PDO went through a strong, downward shift, which – aside from 2003 and 2004 – was largely sustained. Thus, there is some evidence that the 1998 regime shift identified in the current study may be at least partly related to changes in the PDO.

Upon applying the same step-change procedure described in section 2.3 to the PDO, we found significant, decadal-scale changes in the annual PDO, as well as the PDO summer index (PDOs) and winter index (PDOw). Significant upward shifts in all three indices were identified around 1977 and 1926 (which was also a record-low year for Lake Superior water levels), while significant downward shifts were found in 1944 (during a period of relatively high water levels). The PDOs also underwent a significant, downward step-change in 1998, as shown by the solid, horizontal lines in Sup. Figure 3, while the PDOw did not. The annual PDO index also shifted downward in 1998, but the change was only significant at the 85% level. Thus, it can

generally be concluded that the PDO warm phase (associated with colder Great Lakes winters) dominated from 1977 to 1997, while the cold-phase PDO (warmer Great Lakes winters) dominated from 1998 onward. Although the ice cover and NDBC buoy observations used in this study are too short to assess potential decadal changes around 1977, it is noteworthy that the winters of 1976/77 and 1978/79 were the severest on record in terms of ice cover (Figures 3 and 4). Summer water temperatures for 1979 were also below normal (Figure 5).

The potential connections identified here between the PDO and the 1998 Lake Superior regime shift are by no means meant to offer an exhaustive explanation. It is not clear, for example, why a downward shift in the PDO summer index around 1998 (but not the PDOw) might be associated with decreased wintertime ice coverage. Lake Superior is a large, deep lake, and there is strong potential for intrinsic memory in the lake system. Warm summer water temperatures, for example, could lead to delayed ice onset in the winter, similar to how winter ice cover has been proposed to impact summer stratification and water temperature (Austin and Colman 2007). This strong interplay among ice cover, temperature, and evaporation should continue to be investigated as a potential contributing explanation for the 1998 regime shift within the Lake Superior system (including its prolonged, weak "recovery"). On the other hand, there are a multitude of other external climatic factors that should also be examined, including changes in air temperature, cloud cover, humidity, and wind speed – all of which impact water temperature, evaporation, and ice cover to varying degrees. Finally, additional research is needed to examine the ecological implications of the observed step

changes in Lake Superior ice cover and water temperature, as well as whether such regime shifts exist in other lakes and aquatic ecosystems within the Great Lakes region.

CHAPTER 3: CONNECTIONS AMONG LAKE SUPERIOR ICE COVER, EVAPORATION, AND WATER TEMPERATURE

1. Introduction

Changes in regional and global climate have in recent years focused on the effect on large lakes, such as Lake Superior. Interactions among ice cover, water temperature, and evaporation have been explored, but a full understanding has yet to be established. Ice cover has been found to be decreasing worldwide(Anderson 1996, Duguay 2006, Futter 2003, Hanson 1992, Hodgkins 2002, Jensen 2007, Magnuson 2000, Robertson 1992, Wang 2011), and this is expected to coincide with increased evaporation from lake surfaces, as they experience a longer open water season (Assel 2003, Brown and Duguay 2010, Mishra 2010, Wang 2010). Ice cover has also been found to be strongly negatively correlated with the following summer's surface water temperatures (Hanrahan 2010), which are found to be increasing significantly throughout North America (Anderson 1996, McCormick and Fahnenstiel 1999, Schneider 2009). These increases in summertime water temperature in conjunction with smaller trends in air temperature over Lake Superior are suggested to lead to increases in summertime evaporation (Austin and Colman 2007). Additionally, resulting increases in summer wind speed due to the destabilization of the over lake air will work to enhance evaporation (Desai 2009). This "standard paradigm" of decreasing ice cover, increasing water temperatures, and increasing evaporation may not stand as a full explanation of the role of evaporation in these processes.

Additional connections among these surface conditions of the lake, (i.e. water temperature and ice cover) and evaporation have been suggested (Blanken 2011), specifically the negative feedback that evaporation can have on water temperature. More evaporation in the fall before ice cover sets on will cool the lake quicker, leading to an earlier onset of ice cover. This would stand as the opposite interaction than the current thinking (lower ice cover leading to higher evaporation), with higher evaporation leading to higher ice cover. This paper will further explore this effect of evaporation on water temperature and ice cover through time-lagged correlation and composite analyses. The study will include entire years (summer to summer) in order to fully examine the roles and interactions of the three variables.

2. Data and methodology

2.1 Datasets

Data used for this study includes hourly water temperature from three National Data Buoy Center buoys (1979-2010), as well as model estimated "lake-wide mean" surface temperature and evaporation dataset from the National Oceanic and Atmospheric Administration (NOAA) Great Lake Environmental Research Laboratory (GLERL) (taken 1979-2010 for consistency with buoy dataset).

Ice cover records were obtained from the NOAA Great Lakes Ice Atlas for the period 1973-2010. In total, seven different ice metrics were calculated using these roughly bi-weekly composite ice charts. All data quality control and processing is discussed at length in Chapter 1. These include: ice duration, 5% ice-on date, 5% ice-off date, mean and maximum spatial ice extent, date of ice maximum, and ice fractional days (IFD).

2.2 Trend removal

For the analysis portion of this study, any trends in the data must first be removed in order to eliminate biases. For example, two datasets with increasing trends will be correlated, regardless of physical connections between the two. For the correlation analysis and a portion of the composite analysis, trends were removed in the following ways:

The ice data used for this study were previously analyzed for trends, and found to display a large step change between 1997 and 1998. For ice cover, the mean for 1973-1997 was subtracted from that data in that period, and the mean for 1998-2010 was subtracted from the data in the later period in order to remove the step change.

Summer water temperature also exhibited a step change, specifically the months of July, August, and September. For this study, we will only use the months available in both the buoy and GLERL-estimated water temperatures, May-October. The months of May, June, and October also exhibited step changes in 1997/98 significant to at least the p=0.1 level. In order to establish a monthly, detrended water temperature dataset, the monthly means for 1979-1997 and 1998-2010 were removed from the respective periods in each the NDBC and GLERL monthly water temperature datasets.

Evaporation data displayed a step change as well, but only in the months of July and August. For this reason, means from 1979-1997 and 1998-2010 were removed from the respective periods for the months of July and August only. For the

other months which did not show strong linear or nonlinear trends, the mean for the entire period 1979-2010 was subtracted.

2.3 Correlation and Composite Analyses

Correlation analysis was utilized first to assess the connection among ice cover, water temperature, and evaporation. Trends were removed from the data using the process detailed above. All ice cover metrics were correlated with monthly evaporation in the months leading up to, during, and after ice cover. Additionally, ice cover was correlated with water temperature both in the months before ice onset and the months after ice off. By performing this analysis with various time lags, a more comprehensive idea of the connections among the variables can be established.

Composite analysis was also performed to evaluate the connections among ice cover, evaporation, and water temperature. In this case, both the absolute ice data and the data with the step change removed were used. The years 1980-2010 were separated based first on the absolute ice duration timeseries. The highest ten years were classified as high ice years (HIY), the lowest ten years were classified as low ice years (LIY), and the remaining eleven years were classified as intermediate ice years (IIY) (Table 2). These years were used because buoy-measured water temperature data begin in 1979, and the year 1980 in ice the ice record corresponds to the winter of 1979/1980. Using these years, mean water temperature and evaporation were calculated from May before ice cover to October following ice cover. The same process was then perfomed using data with the step change removed as detailed above (Table 3). Detrended data was used so that the year

selection was not biased toward the lower ice cover in recent years and higher ice cover in the beginning of the record. Significance was tested using a Mann-Whitney rank-sum test on each month to determine if data in high and low ice years were from statistically different distributions.

3. Results

3.1 Correlation Analysis

Summer water temperature and ice cover in the following winter do not show a significant correlation. However, summer water temperature exhibits a strong negative correlation with previous winter ice duration, ice off date, mean and maximum ice extent, date of ice maximum, and IFD (Figure 8). Warmer summer water temperatures, both GLERL and NDBC data, occur after both longer ice seasons (ice duration) and those of larger spatial extent (mean, max ice extent). The strongest of these correlations is between water temperature and 5% ice off date, which is significant to the 99% level for May-August for both the GLERL and NDBC datasets (r=-0.88, -0.85, -0.74, -0.62 respectively for the GLERL data and r=-0.88, -0.79, -0.84, -0.74 for the NDBC data). This strong correlation makes physical sense, as longer ice cover (later 5% off date) will lead to a later stratification and therefore cooler temperatures into the summer months.

The only time that the two water temperature datasets show a variance in correlation patterns was between 5% on date and water temperature. For buoy-measured water temperature, no months show a statistically significant correlation, while for GLERL-estimated water temperature, the months of June and August are significant at p=0.05 and the months of May, July, and September are significant at

p=0.1. The GLERL average temperature includes bays and shallower areas, while the buoy averages just three points in the deepest, central parts of the lake. Ice forms first in the bays and shallow portions of the shoreline, so it is not surprising that the correlations with ice-on date are stronger for a dataset including these areas.

Evaporation exhibited strong correlations with ice cover in both the months preceding and following ice cover (Figure 9). Correlations in the months before ice cover represent the time of year when the vast majority of evaporation is occurring, and the strongest correlations occur in the month of December. The 5% ice on date is the highest correlation of all of these, at r=-0.54 (p=0.01). When considering the fundamental effect of ice "capping off" evaporation from the lake, this seems to be contradictory. Higher amounts of evaporation should be correlated with a later 5% ice on date, as the lake would be open for evaporation for a longer amount of time. This metric, however, does not account for complete coverage of the lake, only 5%, which still leaves the majority of the enormous lake surface open to evaporate. If considering the cooling effect that evaporation has on water temperatures, higher evaporation in the month of December would lead to cooler water temperatures and an earlier ice-onset.

The remaining ice metrics further display the connection between ice cover and the cooling effect of evaporation. Again, the highest and most significant correlations occur in December, at the height of the air-water temperature differential over Lake Superior, immediately before ice-on. Duration, 5% off date, and IFD are all significant.

June and July of the summer following ice cover showed substantial negative evaporation-ice cover correlations in nearly all ice metrics. Longer seasons of ice cover limit the amount of evaporation into the spring and summer, keeping water temperatures cooler as the air begins to warm. However, this is also occurring in the months with the lowest amount of evaporation over Lake Superior. Large variations between years in summer evaporation contribute a very small change to annual totals. On the other hand, relatively small changes in fall evaporation can greatly affect amounts of annual evaporation over the lake.

3.2 Composite Analysis

Monthly water temperature averages using absolute water temperature data (before step-change removal) were first calculated for the three groups (HIY,IIY,LIY) for the months of May-October. This included the months in the year before ice cover, as well as those in the year after (Figure 10). During HIY, water temperatures were higher in the months before ice cover and lower in the months following ice cover. However, the months preceding ice cover were not as significant as those in the summer following ice cover. Only the month of October was significant to $p=0.1$. However, nearly all months displayed statistically significant differences between HIY and LIY to $p=0.01$ in the summer following ice cover. This demonstrates, as does the correlation analysis presented earlier, that years with high ice cover correspond to lower water temperatures in the following summer. Additionally, this portion of the composite analysis suggests that a warmer October occurs before years with higher ice cover. This seems somewhat converse of what would be expected, as a cooler summer would presumably correspond with an earlier ice-on date and

therefore a higher ice season. Evaporation can provide the necessary link between warmer water temperature and higher ice cover. Warmer water would lead to a higher amount of evaporation, which would then lead to a higher amount of ice.

Not all months displayed statistically significant differences between HIY and LIY when using NDBC buoy data. August before ice cover was significant to p=0.1, but no others in the summer before ice cover were significantly different. Summer water temperatures in the months after ice cover showed somewhat more significance, with July and August significant to p=0.05, and May significant to p=0.1. As stated earlier, the GLERL average temperature includes bays and shallower areas, while the buoy water temperature averages just three points in the deepest, central parts of the lake. The buoys out in the central part of the lake rarely experience extensive ice cover, as Lake Superior rarely freezes over out to these deep areas. Therefore, buoy water temperature and ice cover would understandably be less connected than the GLERL water temperature and ice cover.

Composite analysis was also performed using water temperature anomaly datasets, or ones with the step changes removed (Figure 11). Again, the largest, most significant differences were seen in the GLERL water temperatures in the months following ice cover, all significant to p=0.01. Water temperatures the summer before HIY were also consistently warmer than those in summers before LIY, though the differences were not as significant. In terms of buoy measured water temperatures, the summer before ice cover again experienced insignificant differences between HIY and LIY. The summer following ice cover showed more significant differences, with the months May, July, and August significant at p=0.01

and June at p=0.05. June and July also experienced differences of over 3°C between HIY and LIY. September and October were insignificant.

The same analysis was also performed on evaporation datasets, both including the step change and with the step change removed (anomalies). During the months immediately before ice cover onset and during the beginning of ice cover on Lake Superior (Nov, Dec, Jan), the difference in evaporation between HIY and LIY is very pronounced (Figure 12). However, these months are not all significant past p=0.1. While the disparity of nearly 1 cm/month in December accounts for approximately 25% change from HIY to LIY, December is quite variable from year to year, and therefore the two datasets, HIY and LIY, are not definitively from different distributions. Nonwithstanding, this amount of evaporation has a very large cooling effect on the lake. As the lake cools rapidly from the evaporative energy leaving the lake, ice cover is able to set on sooner. When the analysis was performed with monthly evaporation anomalies, similar patterns were seen as in the previous analysis with absolute evaporation values (Figure 13). The months of November, December, and January were all significant to at least p=0.1. Evaporation during in the months immediately preceding and during ice formation was much higher in HIY than in LIY. Also, differences in late summer and early fall evaporation after ice cover, specifically September, exhibited higher evaporation in LIY than in HIY, significant to p=0.01.

Converse to the correlation analysis, in which the strength of the connection between ice cover and evaporation tapered off from August to October, the composite analysis shows the largest differences in the late summer and fall. While

June is the only month that shows a significant variability between HIY and LIY during the spring and early summer, the months of September and October are significant to p=0.05 and p=0.1, respectively. This implies that evaporation and ice cover are linked not only in the months bordering ice-on and ice-off, but far into the following season.

4. Discussion and Conclusions

Through correlation and composite analysis, the interactions and connections between evaporation, water temperature, and ice cover have been explored. Specifically, the cooling effect on evaporation has been considered and fit into the puzzle of the annual ice and water temperature cycle of the lake. The "standard paradigm" of higher ice cover corresponding with less evaporation (due to the capping effect of the ice) has been shown to not fully describe the relationship between the two (Figure 14a). Rather, the complex connections between evaporation and ice cover are best understood and described by using a time lag between the datasets.

Higher evaporation in the fall before ice onset cools the lake quicker, which leads to an earlier ice-on date and a larger spatial ice extent during the winter. This is further seen in the composite analysis of water temperature and ice cover. Higher water temperatures occur in the fall before high ice years, enhancing evaporation as instances of cold air increase into the late fall and early winter, and therefore cooling the water to lead into a high ice winter (Figure 14b).

These connections have a solid justification in the physical processes of evaporation and ice cover, but this study has also uncovered connections that are

not so clearly explained. The persistence of these analyses into the following summer and even fall suggest a longer-term connection between the three variables. This could be evidence of a "multi-year lake memory," or interactions that continue between years, not only from season to season. While it is not in the realm of this study to suggest the physical basis in which the lake would respond to previous years, especially considering the multitude of influences acting on Lake Superior, it certainly merits additional study.

The importance of the effect on total annual evaporation also cannot be overlooked in this study. The variation shown between high ice years and low ice years accounts for a large change in not only lake water levels, which lead to other ecological and anthropogenic effects, but also regional climate surround Lake Superior. Directly monitoring these changes in evaporation is difficult, due to the expense and logistical needs for extensive evaporation studies. However, in recent years, the importance of these measurements has led to a few directly-measured evaporation studies over Lake Superior and the other large lakes (Blanken 2000, Blanken 2011, Rouse 2004, Rouse 2008, Spence 2011). Continued effort on this front will also provide additional evaporation datasets to examine, furthering the study of the connections presented in this paper.

CHAPTER 4: VARIABILITY IN SENSIBLE AND LATENT HEAT FLUXES OVER LAKE SUPERIOR: DIRECT OBSERVATIONS FROM A NEARSHORE EDDY COVARIANCE STATION

1. Introduction

Evaporation is an integral component to both the surface energy and water budget of any lake. While its importance is not disputed, it is extremely difficult to directly measure evaporative fluxes, especially on lakes as large as Lake Superior. In many cases, evaporation is estimated as the residual of one of these budgets, both on Lake Superior (Schertzer 1978, Croley 1992, Rouse 2003, Assel 2004, Lenters 2004, Hanrahan 2010), and other lakes worldwide. There are a few direct observations of large lake evaporation using eddy covariance systems over both Great Slave Lake (Blanken 2000, Rouse 2008), Lake Superior (Spence 2011, Blanken 2011), and other lakes worldwide (Assouline and Mahrer 1993).

As the lake continues to adjust to the changing climate, an understanding of the annual and interannual patterns and variability in evaporation is necessary. This study presents data from nearly two years of eddy covariance measurements from a station at Granite Island, MI to investigate this variability. Two winter seasons are included in this timeseries, and comparisons between them are able to shed some light on connections discussed in the previous chapter, as well as possible climatic drivers of evaporation. In addition, comparisons with a similar station located 55km NE of Granite Island, Stannard Rock, serve as a useful comparisons for both evaporation and sensible heat flux as well as other variables measured.

2. Methodology

2.1 Site and Instrument Description

Measurements were taken at a meteorological station installed on Granite Island, MI (N 46°43.226', W 87°24.716'), located 7km from the nearest shoreline and 10 km north from the harbor in Marquette, MI [Map: Figure 15]. The island served as a US Coast Guard light station from its construction in 1868 until the light was automated in 1939. The island was purchased in 2000 by a private citizen, who has undertaken extensive renovations to the lighthouse, tower, and infrastructure. Granite Island is also on the list of National Register of Historic Places (Holman 2011).

The fog bell tower on the island (iron and wood construction, circa 1910) provided a high (approximately 27m above water level) and largely unobstructed location, ideal for installation of an eddy covariance system. Additionally, the privately owned island provided a consistent internet-link for real-time data quality control.

Instrumentation included a LI-7500 open path gas analyzer (LiCor, Lincoln, NE) and CSAT 3D sonic anemometer, mounted facing 280° (Campbell Scientific, Logan, Utah) (Figure 16). Data for this study includes year-round sensible heat and water vapor fluxes measured using the LI-7500 from October 2010-April 2012. In addition, a KH2O krypton hygrometer was used to measure sensible heat and water vapor flux beginning in July 2009. However, for this study, we will be analyzing only the LI-7500 data. Ice cover data was taken from the Canadian Ice Service (www.ice.ec.gc.ca).

2.2 EddyPro Software and Quality Control

Data was processed using EddyPro software, available free of charge from LiCor (Lincoln, NE). This software performs various data processes, including but not limited to: axis rotation, detrending of raw time series, compensation of the lag between the sonic anemometer and gas analyzer, statistical tests for raw time series data (Vickers and Mahrt 1997), compensation for air density fluctuations, (Webb 1980), corrections for frequency response (Moncrieff 1997), and additional quality control tests for fluxes (Foken 2004). Additional information about the functionality and processes included in this software can be found at www.licor.com/eddypro. EddyPro Advanced software was used for this analysis, and all variables were kept as default, except the absolute limits on wind speed were raised to 35 m/s for horizontal wind speeds, and 6 m/s for vertical.

Half-hour averaged output from this program included wind direction and speed, latent and sensible heat flux, and footprint calculations. Daily values of latent and sensible heat flux were calculated for those days which had more than 25% data availability (12 values or more). Seven-day running means were then calculated with these daily values.

3. Results

3.1 Footprint Analysis

The footprint, or the upwind area which the instruments "sense", can also contribute to producing non-stationary data, If the footprint is large and overlaps

any land surface (i.e. shoreline), this can dramatically change the calculated fluxes and contribute to erroneous data. Additionally, if the footprint is too small and comprises too much of the island itself instead of the surrounding water surface, this can also affect data calculations. On average annually, 90% of the calculated flux (x_90%) is from a distance of approximately 2.3 km from the station and the largest contribution of the flux comes from a distance of approximately 0.8 km. This distance is far enough from the station to not include portions of the island, and is not large enough to be affected by shoreline.

However, the footprint size varies greatly throughout the year, specifically between the seasons. The main factors affecting footprint size are the height of the instrument, atmospheric stability, and the type of surface being measured. (Burba and Anderson 2010). The height of the instrument is constant (approx. 27m), so this cannot account for the changes in footprint size. While the lake does change characteristics between seasons and even from hour to hour based on wave height, atmospheric stability has a much greater influence on the footprint size than relatively small changes in the surface being measured. Footprints are larger in the summer, coinciding with more a more stable atmosphere as the lake is cooler than the overlying air (Figure 17). Smaller footprints in the fall and winter can be associated with higher instability due to both the relatively warmer lake and increase in synoptic low pressure systems. While x_90% can be as large as 4km in the summer, this still would not noticeably intersect with land surfaces, as the nearest shore is at a distance of 12km.

3.2 Average and Seasonal Wind Patterns

On an annual basis, the predominant wind directions at Granite Island are northwest and southeast, with the stronger winds mainly from the southeast (Figure 18). This would coincide with the passage of synoptic scale systems, as southeast winds would result from a cyclone located west/southwest of the station, and northwest winds from a cyclone located to the east/northeast. Slightly over 50% of half-hour average wind speeds fall between 4 and 10 m/s, with only about 2% falling above 16 m/s (Figure 18).

These annual patterns are distinctly divided by season, both in terms of wind speed and direction. Fall (OND) and winter (JFM) tend to be much windier, with an average wind speed in winter of 8.25 m/s and 8.32 m/s in the fall compared to 6.45 m/s in spring (AMJ) and 5.84 m/s in summer (JAS) (Figure 19). The notable difference between the summer and winter seasons are the passage of large storms during the fall and winter (often termed the "Gales of November"). These storms have been measured to produce wind gusts over the island of over 30 m/s.

Wind directions vary much more in the fall and winter, paired with higher wind speeds (Figure 19). Southeast and northwest remain predominant, but there are much more instances of northeast windspeeds in the fall and winter as compared to spring and summer, which could again be associated with the passage of a synoptic system (center located to the southeast of the island). In the spring and summer, there are two predominant wind speeds, northwest and southeast, with a notable lack of variance in other directions. Southeast winds would constitute a "land breeze" off of the Upper Peninsula, which would occur often in the summer

during clear, calm evenings when the land surface cools faster than the lake surface. Land breezes would be associated with much lower wind speeds from the southeast than the passage of a synoptic system, and this is visible in comparing seasonal wind roses (Figure 20). It should be noted that there are very few times when the winds are coming from the direct west. A direct west wind could influence measurements of sensible and latent heat flux, as the instruments could easily pick up signals from the nearby shore. However, because the instance of west wind directions are so low, in addition to the average size of the footprint mentioned in the previous section, we did not directly test for this in our calculations.

3.3 Annual Cycle of and Controls on Latent and Sensible Heat Fluxes

As with other high latitude large lakes, there is a lag between the highest amount of energy input (i.e. summer radiation) and the highest amount of heat release (i.e. fall and early winter evaporative fluxes) over Lake Superior. This is due mainly to the high specific heat content of the deep lake. The largest amounts of evaporation occur in the fall and early winter (September – December) and drop off sharply as the lake cools and ice cover sets on.

In the beginning of this "evaporation season," LE greatly exceeds H, but by late December or early January, these are reversed and H exceeds LE (Figure 21). This can be explained by a simple saturation vapor pressure curve (Figure 22). As temperatures cool, an equal change in vapor pressure corresponds to a greater change in temperature. Once temperatures are below 0°C (as they are later in winter), vapor pressure changes very little with a change in temperature. As the

difference between the saturated water surface vapor pressure and that in the air vary less, evaporation decreases. Temperatures between the air and water surface, however, can continue to be large, as air temperatures dip below 0°C, allowing for sustained if not increased sensible heat flux.

Evaporation and sensible heat flux are episodic throughout the year. Based on 7-day running averages, there are periods of approximately ten days where fluxes increase and then drop back off (Figure 21). The drivers of these events are mainly the passing of synoptic storm systems. Cold, dry air coming down from the Canadian continental climate meets the relatively warm lake and produces strong vapor pressure gradients away from the lake in addition to high winds. This creates large "pulses" of evaporation, with daily averages during these storms reaching well over 300 W m^{-2}. Sensible heat flux reaches its largest values later in the winter, as discussed earlier. It is strongly paired with evaporation temporally, but its maximum fluxes tend to be a bit lower (maximum daily value of 296 Wm^{-2}, 1/19/2012).

In comparison, both latent and sensible heat fluxes are small, and more often negative, in the spring and summer. Waters warm slowly in the spring, with air temperatures rising relatively quicker. Therefore, by April sensible heat flux often becomes negative, with evaporation hovering close to 0 or slightly below because of the small vapor pressure gradient between the cold water and cool air. Negative evaporation events occur later in the summer as the air warms and creates a stronger vapor pressure gradient toward the lake.

Controls on latent and sensible heat flux vary slightly between events, but there are a few drivers that are ever present. Higher wind speeds lead to greater fluxes, as do larger differences in air and water temperature and vapor pressure. Therefore, it is not surprising that wind speeds vary in concert with H and LE (Figure**s** 23a and b). As stated earlier in this section, H begins to exceed LE once temperatures drop below 0°C in the winter, and this is evident in comparing Figures 23 a and c. Changes in sensible heat flux are tied to changes in air temperature, especially because the temperature of the water changes slower than the variations in air temperature. In terms of evaporation, changes in vapor pressure of the air (Figure 23d) can also affect the amount of evaporation occurring, but the best estimate may be a combination of the two.

Blanken (2011) found that the best estimate for their station at Stannard Rock was to create a linear regression of windspeed divided by the vapor pressure of the air (U/e_a). Using 0,5-hour data, a similar comparison was performed with Granite Island using data from October 6, 2010 – September 30, 2011. The two equations found to best estimate Stannard Rock were 2008/09: $LE=2.51*(U/e_a)-1.27$, correlation coefficient = 0.55 and 2009/10: $LE = 3.31*(U/e_a)-2.25$, correlation coefficient = 0.52. The comparison with U/e_a was not as robust at Granite Island, as the correlation coefficient was only 0.11 (Figure 24). In fact, estimating evaporation using only wind speed produced a slightly higher correlation coefficient (0.12). In order to create a better modeled dataset, it would be beneficial to incorporate water temperature data to find the saturation vapor pressure of the water surface, and

from that it would be possible to calculate the vapor pressure gradient from the water surface to the air.

3.4 Interannual Variability of Latent Heat Fluxes

The data presented in this paper allows comparison of two distinct fall/winter evaporation seasons. In order to have analogous time periods, the dates October 6 – April 23 are defined as the "evaporation season" for this study. In both years, ice cover was very limited. In 2010/11 the maximum ice cover was only 31% over the lake, and in 2011/12 it was only 10%. Because of the nature of the way ice forms on the lake (beginning in shallow areas and bays), this would mean that the waters surrounding Granite Island were likely ice free for the majority if not entirety of both seasons. On average, 2010/11 was a colder year than 2011/12, contributing to a higher amount of sensible heat flux, but the two years on average were otherwise remarkably similar (Table 4).

While the two years look very similar in average values, there were distinct differences in temporal variability that contributed to two very different winters. Variability in cumulative evaporation for the season is mainly due to different timing and intensity of storm systems passing over the lake (Figure 25). There are five distinct periods when comparing the two winters of evaporation, the first lasting from October 6-November 15. Air temperatures were remarkably similar between the two years, varying by only 0.2°C. Average wind speed for this period for 2010/11 was 8 m/s, while average wind speed in 2011/12 was 8.4 m/s. Until

November 15, evaporation totals between the two years traded off, without one being significantly higher than the other.

During the period November 16-December 16, cumulative evaporation in 2010/11 increased greatly in comparison to the following year. The greatest difference between the two years occurred at the end of this period, approximately 45mm. Air temperatures were nearly 2°C colder in 2010/11, and wind speeds were 2.7m/s faster on average. Evaporation rates were also consistently higher in 2010/11 than in 2011/12 during this period. However, in the short time from December 17-January 3, cumulative evaporation in 2011/12 nearly caught up to that in 2010/11. This approximately two week period in 2011/12 had faster winds of 1.7 m/s, but air temperature was about equal to that of 2010/11. Evaporation rates were consistently higher during this time period in 2011/12.

The time from January 4 – February 14 marked another slight divergence of cumulative evaporation rates. Air temperatures were over 4°C cooler in 2010/11, and wind speeds were slightly higher. During the time period after February 14, evaporation in 2010/11 leveled off, while that in 2011/12 continued to increase for the rest of the season. This coincides with the period over which ice set on to the lake in 2010/11, whereas 2011/12 stayed mostly ice free. This limited the amount of evaporation occurring in 2010/11, allowing cumulative evaporation to end with only 3% difference between the two seasons.

On a monthly basis, evaporation from October 6-31 varied between the two years (95mm in 2010, 83mm in 2011), mainly due to a large evaporation event from

October 17-21, 2010, producing 37mm of evaporative water loss. November air temperatures and evaporation were very similar between the two years, averaging 4.4°C 2010/11 and 4.5°C in 2011/12. However, evaporation was higher in 2010/11 (122mm) than 2011/12 (105mm).

December temperatures were 1.5°C cooler in 2010 than in 2011, but interestingly, December 2010 measured 121mm compared to 135mm of evaporative water loss in 2011. Additionally, December 2010 was windier than 2011, with an average of 9.4 and 8.4 m/s respectively. January was much colder in 2011 (-6.4°C) than 2012 (-2.9°C). Interestingly, January, despite its relatively large temperature difference between the two years, varied less than December, from 117mm in 2011 to 114 mm in 2012. During this fall and early winter season, evaporation was higher in 2010/11, and as stated earlier, the difference between the cumulative evaporation in both years peaked in mid December at 45mm.

The remainder of the evaporation season (FMA) showed, as expected, lower amounts of evaporation in both years than the months of October-January. However, rates were higher in 2011/12 than in the previous year. February 1-April 23 evaporation measured 99mm in 2011 compared to 110mm in 2012. It should be noted that there was a power outage to the station February 27-March 1, 2012, so this amount of evaporation may be an underestimation due to those missing data points. By the end of the season, evaporative losses were slightly higher (18mm) in 2010/11 than in 2011/12, but this only represents a 3% difference when considering the cumulative evaporation of 553mm in 2010/11 and 546 mm in

2011/12. While 2010/11 began as a much higher evaporation year, 2011/12 caught up with higher totals in the later part of the winter.

As stated previously, evaporation during the remaining months of the year (May-September) is generally low and at times negative (i.e. condensation). The period from April 24, 2011 – October 5, 2011 measured 227mm over the approximately 5.5 month period. Interestingly, however, there was a very large evaporative event, in fact the largest in our record, which occurred from September 13-18, contributing 47mm of evaporation, or 21% of the evaporation in this period. This is an early instance of an event this large, as these do not on average occur until later in the season when the air temperatures have cooled significantly as compared to the lake surface. Whether this was an anomalous event or a trending toward an earlier beginning to the evaporation season remains to be seen. An increase in summer (JAS) evaporation and decrease in winter evaporation (Nov/Dec) seen in Lake Superior data from 1948-1999 (Lenters 2004) may support this theory.

3.5 Comparison to an Offshore Lake Superior Eddy Covariance Station (Stannard Rock)

A similar measurement site located at Stannard Rock Light, 55km NE of Granite Island (Figure 26), provides a convenient and useful comparison to the analysis being performed at Granite Island (Blanken 2011). Differences between the two stations can be found in the lower half Table 3. Stannard Rock's instrumentation is slightly higher (32.4m vs 27.2 at Granite Island). Additionally, the station is located farther out in the lake and the average water depth at Stannard is not surprisingly higher, 136.5m to 74.0m at Granite Island (data from the National

Geophysical Data Center; http://www.ngdc.noaa.gov/mgg/greatlakes/superior.html). Due to these deeper waters surrounding Stannard Rock, the water temperatures are generally colder. Because of this, stability tends to be higher at Stannard Rock, increasing the size of the flux footprint from that at Granite Island. Peak flux footprint distance is somewhat similar (674 at Stannard, 818 at Granite), but the x_80% distance is significantly larger at Stannard (6km) than Granite (2km). Also due to site location and height of instruments, Stannard Rock tends to be slightly windier. Average air temperature at Granite Island in 2010/11 is very similar to that at Stannard Rock in 2009/10. Average latent heat flux is slightly higher in 2010/11 than 2009/10 at Stannard, and significantly higher than 2008/09 (Table 4). The differences, however, are not significant enough to be considered outside the realm if interannual variability.

4. Discussion and Conclusions

The two years of data collected from Granite Island provide insight to both seasonal and interannual patterns of latent and sensible heat fluxes. The data illustrate the sharp increase in evaporation in the fall/winter, as well as the temporal tradeoff between latent and sensible heat fluxes as the winter season progresses. In addition, large evaporative flux events were recorded, with an early season evaporation of 47mm total from September 13-18, 2012, the largest in the record.

There are many climactic and limnological drivers of evaporation, all working in concert to influence its variability. This study found that among air temperature, vapor pressure of the air, and wind speed, the best estimation of evaporation through linear regression was with wind speed alone. In contrast, Blanken [2011] found the best agreement with lake evaporation measured at Stannard Rock to be U/e_a. Incorporating surface water temperature in modeling evaporation would be a sensible next step in this endeavor, since water temperature often plays an equally significant role in the variability of evaporation, as compared to the humidity of the air.

The two winters summarized in this chapter experienced very similar amounts of cumulative evaporation from October-April (only varying by 3%), but the maximum ice cover extent of the lake varied between the two years by more than a factor of three (31% compared to 10%). This contrasts with the "standard paradigm" presented in chapter 3, as the almost equal amounts of evaporation during the winter coincided with very different amounts of ice cover. Furthermore, the more complex connections presented in chapter 3 are observable in the two years of data from Granite Island.

While cumulative evaporation was nearly equal between the two years, evaporation was not equal at all times throughout the winter. The fall and early winter of 2010/11 experienced higher evaporation than the same period in the following year, and this coincides with higher ice cover during the 2010/11 winter. On the other hand, evaporation in the late winter and early spring of 2011/12 was

higher following the very minimal amount of ice cover on the lake that year. The summer of 2011 was warm, but not anomalous as compared to the previous five years. In contrast, at the time of this publication (summer 2012), Lake Superior is on track to experience a record-warm summer. Water temperatures began rising in early March, with a previously unobserved brief stratification in late March. Water temperatures as of late July are nearly five degrees higher than the 1992-2011 average. In concert with this, the lake is beginning to evaporate much earlier than average. This can be seen in the real-time evaporation data coming from Granite Island, as well as in the leveling off of water temperatures usually seen in late August and early September, as evaporative cooling increases (Figure 27). As this feedback continues, it will be interesting to observe whether water temperatures drop off precipitously earlier in the year in 2012. The low ice cover experienced in 2011/12 has indeed corresponded to higher summer water temperature as well as a remarkably early start to the "evaporation season."

As monitoring stations continue to operate over and around the waters of Lake Superior, a greater understanding of the physical connections among ice cover, evaporation, and water temperature will develop. By collecting *in situ* evaporation data, patterns and trends seen in the historical (i.e., modeled) data can be explored to determine how pervasive the connections discussed in this thesis are present in observational data.

CHAPTER 5: SUMMARY AND FUTURE RESEARCH

This study has highlighted both changes in and interactions among Lake Superior ice cover, evaporation, and water temperature. In terms of long-term trends, it was discovered that linear regression methods are not appropriate for accurately describing the changes that have occurred in recent decades. Rather, the majority of the long-term "trends" seen in previous studies of ice cover, water temperature, and evaporation are actually due to a pronounced step-change that occurred in 1997/98. During the El Niño winter of 1997/98, record low ice cover was recorded over the lake, followed by record-warm summer water temperatures in 1998, as well as near-record July/August (JA) evaporation. This step-change defines two separate climatic regimes, defined by a 40-day drop in ice cover duration, 3°C increase in summer water temperature, and near doubling of summer evaporation from the early to the later period.

The fact that this step-change is coherent across all three variables suggests connections among ice cover, evaporation, and water temperature on decadal timescales. Through correlation and composite analysis, we determined that similar connections exist on seasonal to interannual timescales. Specifically, high evaporation in the fall is often associated with higher ice cover during the following winter, which then leads to a cooler summer and lower evaporation rates. Thus, one cannot simply assume the "standard paradigm" in which high (low) ice cover leads to low (high) evaporation. While this may be true in late winter, when ice cover presents a physical barrier to surface evaporation, the results presented here paint

a much more complex picture when considering total annual evaporation. In particular, we find that extensive ice coverage – rather than being simply a barrier to winter evaporation – may, in fact, be indicative of higher evaporation rates during the preceding fall season. This suggests that any water "savings" provided by high ice cover during the winter (as well as reduced evaporation during the following summer, in conjunction with lower water temperatures) may be significantly offset by higher fall evaporation rates that led to the increased wintertime ice cover in the first place. Future studies of these interactions should carefully consider such seasonal lags and feedbacks when determining the impacts of ice cover on total annual evaporation.

While these connections are seen across the historical record, on both decadal and interannual timescales, there are very few direct measurements of evaporation over Lake Superior. This necessitated the use of a 1-D thermodynamic model for estimating historical evaporation rates for much of the work presented in this thesis. To address this gap, the final chapter of the study presented data from an eddy covariance station on Granite Island, Michigan. Despite the intensive nature of the measurement technique, two full winters of data were available for this study, allowing for analysis of both the seasonal and interannual variability. On a seasonal basis, we observed an increase in sensible heat flux from low levels in the fall and early winter to higher rates that eventually exceeded latent heat flux by mid winter. Episodic events with large latent heat flux were also observed, sometimes reaching daily averages of over 300 W m^{-2} (i.e., evaporation rates of ~1 cm day^{-1}). Similar to the 1-D model results, interannual comparisons between the winters of 2010/11

and 2011/12 showed that large amounts of evaporation in the fall and early winter of 2010/11 coincided with higher ice cover later that winter. The winter of 2011/12, on the other hand, showed higher evaporation rates in mid winter and early spring in association with the record-low ice coverage that year, and this resulted in a difference of only 3% in cumulative evaporation between the two study years.

The similar values of cumulative evaporation between the two years contrasts with the "standard paradigm" that is often assumed – namely that greater ice cover corresponds to lower evaporation rates. Furthermore, the difference in timing of the largest amounts of evaporation between the two years support the connections described in chapter three, which showed that higher fall evaporation was typically associated with higher ice cover later that winter. The summer of 2011/12 has also been remarkably warm as of mid July, which matches the connections discussed in chapter three between low ice cover and warm summer water temperatures. In addition, evaporation has already begun to increase on Lake Superior (as measured at Granite Island and also evidenced by a leveling off of surface temperatures), and this is considerably earlier than usual. How this pattern will continue to evolve into the winter of 2012/13 remains to be seen, but the results of the current study suggest the likelihood for strong evaporative cooling during the fall, which may lead to a stronger-than-normal drop in water temperature and a possible return to more normal ice cover.

Further study is needed to determine if the strong interplay among ice cover, temperature, and evaporation is a potential contributing explanation for the 1997/98 regime shift within the Lake Superior system. There are also a multitude of other external climatic factors that should also be examined in the context of this regime shift and the connections among ice cover, water temperature, and evaporation. These include changes in air temperature, cloud cover, humidity, and wind speed – all of which impact each of these three variables to some degree. Additional research is also needed to examine the ecological implications of the observed step changes in Lake Superior ice cover and water temperature, as well as whether such regime shifts exist in other lakes and aquatic ecosystems within the Great Lakes region. The importance of *in situ* evaporation measurements is paramount for monitoring ongoing and future changes in Lake Superior, as well as in other large lakes worldwide. Increased understanding of the complex drivers of evaporation will inform and improve predictive models and provide water resource managers with valuable information for assessing the impacts of climate variability and change on evaporative water loss and lake levels.

APPENDIX A: REFERENCES

Anderson, W. L. e. a. (1996) Evidence of recent warming and El Niño-related variations in ice breakup of Wisconsin lakes. *Limnology and Oceanography,* 41**,** 815-821.

Assel, R. A. (1998) The 1997 ENSO event and implication for North American Laurentian Great Lakes winter severity and ice cover. *Geophysical Research Letters,* 25**,** 1031-1033.

---. 2005. Great Lakes ice cover climatology update: Winters 2003, 2004, and 2005*.,* ed. NOAA. Ann Arbor, MI.

Assel, R. A., et al. (2003) Recent Trends in Laurentian Great Lakes Ice Cover. *Climatic Change,* 57**,** 185-204.

Assel, R. A. & D. M. Robertson (1995) Changes in winter air temperatures near Lake Michigan, 1851-1993, as determined from regional lake-ice records. *Limnology and Oceanography,* 40**,** 165-176.

Assel, R. A. e. a. (2004) Hydroclimatic factors of the recent record drop in Laurentian Great Lakes water levels. *Bulletin of the American Meteorological Society***,** 1143-1151.

Assouline, S. & Y. Mahrer (1993) Evaporation from Lake Kinneret: 1. Eddy correlation system measurements and energy budget estimates. *Water Resour. Res.,* 29**,** 901-910.

Austin, J. A. & S. M. Colman (2007) Lake Superior summer water temperatures are increasing more rapidly than regional air temperatures: A positive ice-albedo feedback. *Geophysical Research Letters,* 34.

Blanken, P. D. e. a. (2000) Eddy covariance measurements of evaporation from Great Slave Lake, Northwest Territories, Canada. *Water Resources Research,* 36**,** 1069-1077.

--- (2011) Evaporation from Lake Superior: 1. Physical controls and processes. *Journal of Great Lakes Research,* 37**,** 707-716.

Brown, L. C. & C. R. Duguay (2010) The response and role of ice cover in lake-climate interactions. *Progress in Physical Geography,* 34**,** 671-704.

Burba, G. G. & D. J. Anderson. 2010. *A Brief Practical Guide to Eddy Covariance Flux Measurements: Principles and Workflow Examples for Scientific and Industrial Applications*. Lincoln, NE: LI-COR Biosciences.

Croley, T. E. (1992) Long-Term Heat Storage in the Great Lakes. *Water Resources Research,* 28**,** 69-81.

Croley, T. E. & R. A. Assel (1994) A one-dimensional ice thermodynamics model for the Laurentian Great Lakes. *Water Resour. Res.,* 30**,** 625-639.

Croley, T. E., II (1989) Verifiable evaporation modeling on the Laurentian Great Lakes. *Water Resour. Res.,* 25**,** 781-792.

Desai, A. R. e. a. (2009) Stronger winds over a large lake in response to a weakening air-to-lake temperature gradient. *Nature Geoscience*.

Duguay, C. R. e. a. (2006) Recent trends in Canadian lake ice cover. *Hydrological Processes,* 20**,** 781-801.

Foken, T. e. a. 2004. Post-field quality control. In *Handbook of micrometeorology: A guide for surface flux measurements.,* ed. X. L. e. al, 81-108. Dordrecht: Kluwer Academic.

Futter, M. N. (2003) Patterns and trends in southern Ontario lake ice phenology. *Environmental Monitoring and Assessment,* 88**,** 431-444.

Ghanbari, R. N. & H. R. Bravo (2008) Coherence between atmospheric teleconnections, Great Lakes water levels, and regional climate. *Advances in Water Resources,* 31**,** 1284-1298.

Ghanbari, R. N. e. a. (2009) Coherence between lake ice cover, local climate, and teleconnections (Lake Mendota, Wisconsin). *Journal of Hydrology,* 374**,** 282-293.

Hanrahan, J. e. a. (2010) Connecting past and present climate variability to the water levels of Lakes Michigan and Huron. *Geophysical Research Letters*.

Hanson, H. P. e. a. (1992) Recent Great Lakes Ice Trends. *Bulletin of the American Meteorological Society,* 73**,** 577-584.

Hodgkins, G. A. e. a. (2002) Historical changes in lake ice-out dates as indicators of climate change in New England, 1850-2000. *International Journal of Climatology,* 22**,** 1819-1827.

Holman, S. 2011. Granite Island Light Station - Lake Superior.

Hunter, R. S. & T. E. I. Croley. 1993. Great Lakes monthly hydrologic data. In *NOAA Data Report ERL GLERL*. Springfield, VA: National Technical Information Service.

Jensen, O. P. e. a. (2007) Spatial analysis of ice phenology trends across the Laurentian Great Lakes region during a recent warming period. *Limnology and Oceanography,* 52**,** 2013-2026.

Lenters, J. D. (2004) Trends in the Lake Superior Water Budget Since 1948: A Weakening Seasonal Cycle. *Journal of Great Lakes Research,* 30**,** 20-40.

Magnuson, J. J. e. a. (2000) Historical trends in lake and river ice cover in the Northern Hemisphere. *Science,* 289**,** 1743-1746.

McCormick, M. J. & G. L. Fahnenstiel (1999) Recent climatic trends in nearshore water temperatures in the St. Lawrence Great Lakes. *Limnology and Oceanography,* 44**,** 530-540.

Mishra, V. e. a. (2010) Changing thermal dynamics of lakes in the Great Lakes region: Role of ice cover feedbacks. *Global and Planetary Change*.

Moncrieff, J. B. e. a. (1997) A system to measure surface fluxes of momentum, sensible heat, water vapour, and carbon dioxide. *Journal of Hydrology,* 188-189**,** 569-611.

Robertson, D. M. e. a. (1992) Lake ice records used to detect historical and future climatic changes. *Climatic Change,* 21**,** 407-427.

Rodionov, S. & R. A. Assel (2003) Winter severity in the Great Lakes: a tale of two oscillations. *Geophysical Research Letters,* 36.

Rouse, W. R. e. a. (2003) Interannual and Seasonal Variability of the Surface Energy Balance and Temperature of Central Great Slave Lake. *Journal of Hydrometeorology,* 4**,** 720-730.

--- (2004) The Role of Northern Lakes in a Regional Energy Balance. *Journal of Hydrometeorology,* 6**,** 291-305.

--- (2008) An Investigation of the Thermal and Energy Balance Regime of Great Slave and Great Bear Lakes. *Journal of Hydrometeorology,* 9**,** 1318-1333.

Schertzer, W. M. (1978) Energy Budget and Monthly Evaporation Estimates for Lake Superior, 1973. *Journal of Great Lakes Research,* 4**,** 320-330.

Schneider, P. & S. Hook (2010) Space observations of inland water bodies show rapid surface warming since 1985. *Geophysical Research Letters,* 37.

Schneider, P. e. a. (2009) Satellite observations indicate rapid warming trend for lakes in California and Nevada. *Geophysical Research Letters,* 36.

Spence, C. e. a. (2011) Evaporation from Lake Superior 2: Spatial distribution and variability. *Journal of Great Lakes Research,* 37**,** 717-724.

Vickers, D. & L. Mahrt (1997) Quality control and flux sampling problems for tower and aircraft data. *Journal of Armospheric and Oceanic Technology,* 20**,** 143-151.

Wang, J. e. a. (2010) Severe ice cover on Great Lakes during winter 2008-2009. *EOS, Transactions, American Geophysical Union,* 91**,** 41-42.

--- (2011) Temporal and spatial variability of Great Lakes ice cover, 1973-2010. . *Journal of Climate*.

Webb, E. K. e. a. (1980) Correction of flux measurements for density effects due to heat and water vapour transfer. *Quarterly Journal of the Royal Meteorological Society,* 106**,** 85-100.

APPENDIX B: TABLES AND FIGURES

Table 1: Statistical significance (i.e., p-values) of the difference in means for adjacent 10-year periods within the 20-year moving window of the step-change analysis. Years refer to the start of the second 10-year period (and the latter portion of the winter season for the ice metrics). Changes marked with a single (double) asterisk are significant at the 95% (99%) level, with gray shading denoting the year with the most significant step change.

	JAS water temperature		**JA evap.**	**Ice metrics**						
	NDBC	**GLERL**	**GLERL**	**IFD**	**5% ice-on**	**5% ice-off**	**Duration**	**Mean f_{15}**	**Max f_{15}**	**Date of Max f_{15}**
1983		0.031*	0.011*	0.385	0.677	0.045*	0.496	0.273	0.427	0.519
1984		0.104	0.026*	0.521	0.384	0.045*	0.677	0.427	0.623	0.185
1985		0.212	0.014*	0.850	0.426	0.088	0.677	0.791	0.623	0.733
1986		0.140	0.038*	0.273	0.909	0.121	0.364	0.241	0.307	0.705
1987		0.212	0.140	0.121	0.382	0.211	0.427	0.121	0.162	0.289
1988		0.910	0.521	0.791	0.790	0.970	0.734	0.734	0.734	0.049*
1989	0.406	0.850	0.970	0.791	0.595	0.970	0.734	0.623	0.850	0.058
1990	0.762	0.734	0.850	0.623	0.425	0.850	0.940	0.521	0.734	0.272
1991	0.571	0.734	0.910	0.427	0.030*	0.820	0.705	0.521	0.623	0.570
1992	0.473	0.791	1.000	0.385	0.088	0.970	0.880	0.385	0.345	0.733
1993	0.345	0.623	0.970	0.307	0.007**	0.940	0.290	0.345	0.307	0.940
1994	0.162	0.427	0.910	0.571	0.005**	0.970	0.273	0.521	0.473	1.000
1995	0.089	0.186	0.623	0.140	0.003**	0.472	0.104	0.140	0.140	0.705
1996	0.089	0.140	0.307	0.212	0.025*	0.650	0.186	0.273	0.212	0.762
1997	0.014*	0.021*	0.054	0.054	0.015*	0.199	0.031*	0.076	0.054	1.000
1998	0.002**	0.001**	0.001**	0.005**	0.004**	0.010*	0.002**	0.009**	0.007**	0.198
1999	0.007**	0.003**	0.007**	0.026*	0.009**	0.075	0.013*	0.064	0.054	0.520
2000	0.049*	0.031*	0.038*	0.212	0.037*	0.427	0.112	0.427	0.345	0.910
2001	0.140	0.089	0.140	0.427	0.150	0.734	0.290	0.623	0.571	0.850

Table 2: Winter study periods arranged by high ice year (HIY), intermediate ice year (IIY), and low ice year (LIY). Divisions are based on absolute ice duration, with HIY including the top ten years, LIY including the bottom ten, and IIY including the eleven remaining years. Averages for each group are calculated and shown at the bottom of the table.

LOW ICE YEARS		INTERMEDIATE ICE YEARS		HIGH ICE YEARS	
Year	Ice Duration	Year	Ice Duration	Year	Ice Duration
2005/06	29	1979/80	90	1989/90	118
2001/02	34	2007/08	90	1981/82	121
1997/98	35	1982/83	91	1985/86	121
1986/87	47	2004/05	91	1988/89	122
1999/2000	50	1990/91	97	1996/97	122
2009/10	64	1992/93	102	2008/09	123
2006/07	70	2002/03	102	1993/94	125
1998/99	75	1987/88	104	1983/84	128
1994/95	77	2000/01	109	1991/92	133
2003/04	84	1984/85	114	1995/96	136
		1980/81	116		
AVG	56.5	**AVG**	100.6	**AVG**	124.9

Table 3: Winter study periods arranged by high ice year (HIY), intermediate ice year (IIY), and low ice year (LIY). Divisions are based on ice duration anomalies (i.e., with the mean of the two periods, 1979-1997 and 1998-2010, removed from each year during the respective period). HIY includes the top ten ice years, while LIY includes the bottom ten, and IIY includes the eleven remaining years. Averages for each group are calculated and shown at the bottom of table.

LOW ICE YEARS		INTERMEDIATE ICE YEARS		HIGH ICE YEARS	
Year	Ice Duration	Year	Ice Duration	Year	Ice Duration
1986/87	-65.32	2009/10	-9.54	2008/09	49.46
2005/06	-44.54	1987/88	-8.32	2000/01	35.46
2001/02	-39.54	2006/07	-3.54	2002/03	28.46
1997/98	-38.54	1998/99	1.46	199596	23.68
1994/95	-35.32	1984/85	1.68	1991/92	20.68
1999/2000	-23.54	1980/81	3.68	2004/05	17.46
1979/80	-22.32	1989/90	5.68	2007/08	16.46
1982/83	-21.32	1981/82	8.68	1983/84	15.68
1990/91	-15.32	1985/86	8.68	1993/94	12.68
1992/93	-10.32	1988/89	9.68	2003/04	10.46
		1996/97	9.68		
AVG	-31.6	**AVG**	2.5	**AVG**	23.0

Table 4: Comparison of data collected at Stannard Rock to observations at Granite Island. Annual averages are October 1 – September 30 for Stannard Rock Light (Blanken 2011) and October 6 – September 30 for Granite Island. Winter averages are also calculated for two seasons at Granite Island, covering the period October 6 – April 23. Station and footprint values from Granite Island and Stannard Rock are compared in the lower portion of the table.

	Annual Averages			**Winter Averages**	
	Granite Island	Stannard Rock		Granite Island	
	2010-2011	2008-2009	2009-2010	2010-11	2011-12
Avg. LE [W m-2]	61.2	49.4	57.1	78.4	79.1
Total E [mm]	773	464	645	553	546
H [W m^{-2}]	34.2	40	30.8	59.2	42.9
T_a [°C]	6.57	5.07	6.59	0.14	2.63
e_a [kPa]	1.00	0.82	0.89	0.59	0.71
U [m s^{-1}]	7.23	8.91	8.78	8.27	8.16
Instrument height [m]	27.2	32.4			
Water Depth [m]	74.0	136.5			
x_peak [m]	818	674			
x_80% [km]	2.0	6.0			

Table 5: Summary of average conditions (sensible and latent heat flux, wind speed, air temperature, and vapor pressure) in separate winter periods as show in Figure 25.

	Period 1 10/6 - 11/15		Period 2 11/16 - 12/16		Period 3 12/17 - 1/3		Period 4 1/4 - 2/10		Period 5 2/11 - 4/23	
	2010/11	2011/12	2010/11	2011/12	2010/11	2011/12	2010/11	2011/12	2010/11	2011/12
H [W m^{-2}]	20.3	16.5	114.6	77.4	63.9	84.1	105.5	74.2	31.8	14.5
LE [W m^{-2}]	101.7	92.2	144.4	117.8	73.1	133.3	103.2	80.0	25.0	38.8
U [m/s]	8.0	8.4	10.7	8.0	7.7	9.4	8.4	9.0	7.5	7.3
T_a [°C]	9.3	9.1	-1.3	0.5	-1.6	-1.5	-6.5	-2.1	-0.5	3.4
e_a [kPa]	0.9	1.0	0.54	0.59	0.52	0.53	0.38	0.53	0.56	0.73

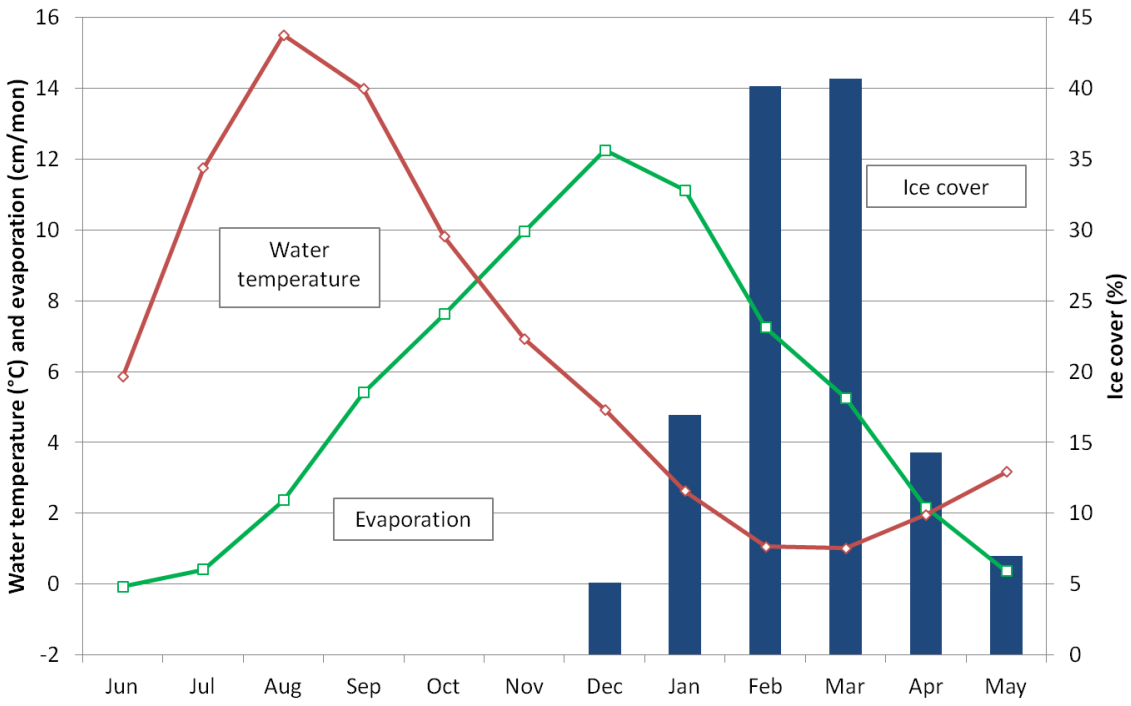

Figure 1: Mean annual cycle of Lake Superior monthly mean water temperature (red line), evaporation rate (green line), and ice cover (blue bars) for the period 1973-2010. Data obtained from Great Lakes Environmental Research Laboratory (GLERL).

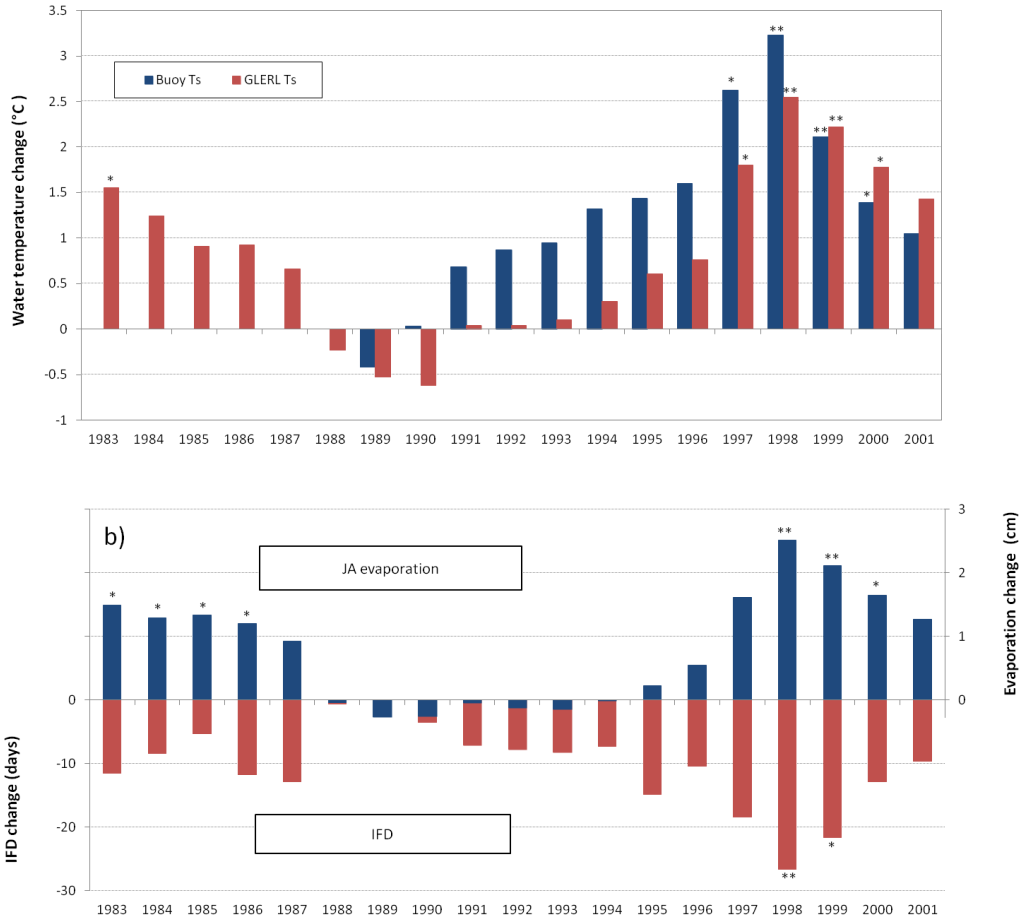

Figure 2: Change in decadal means (second half minus first half) within a 20-year moving window for Lake Superior (a) July, August, September (JAS) surface water temperature, T_s, and (b) winter ice-fractional days (IFD) and July, August (JA) evaporation. Years refer to the start of the second 10-year period (and the latter portion of the winter season for IFD). Single (double) asterisk denotes statistical significance at the 95% (99%) level.

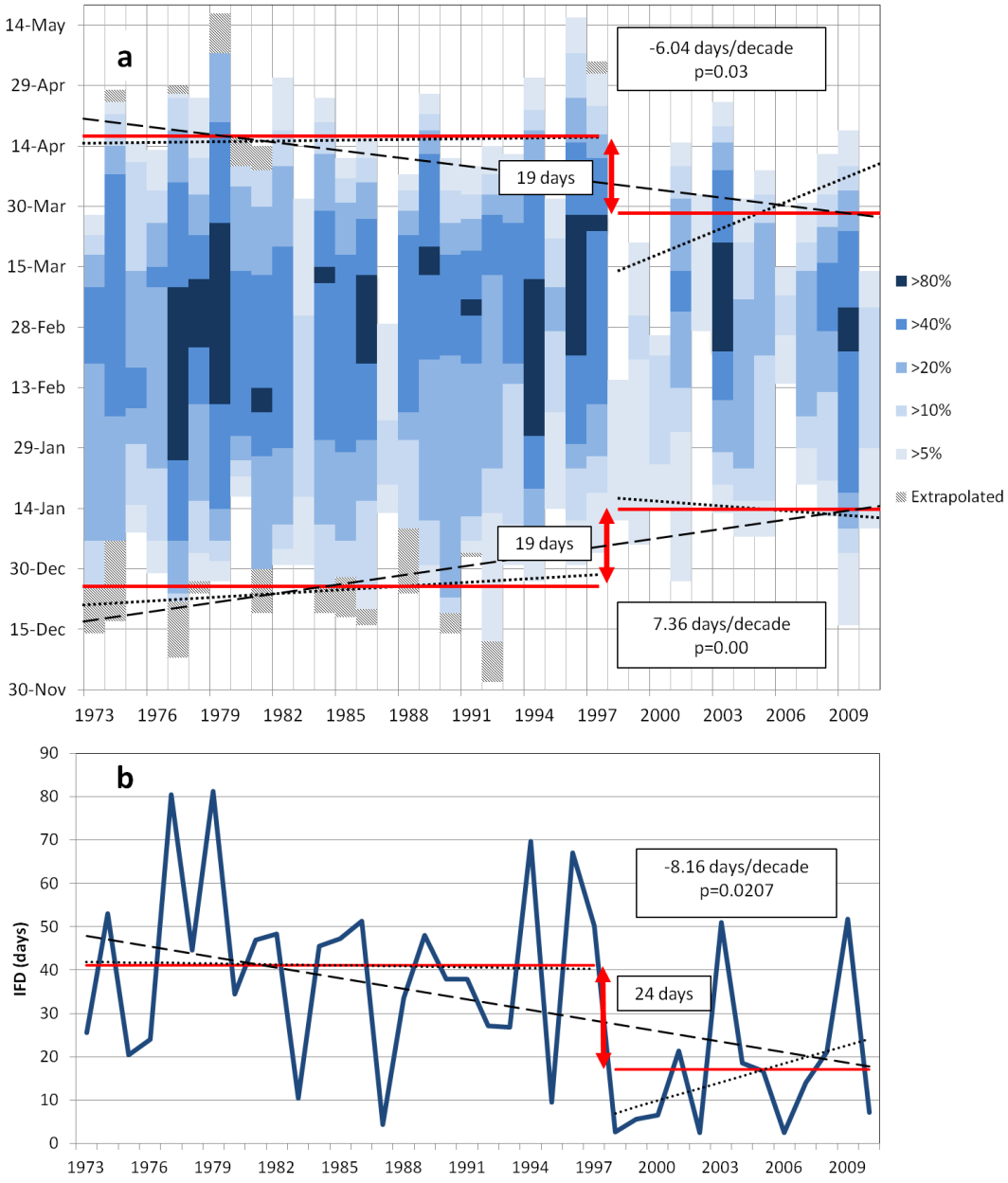

Figure 3: (a) Lake Superior fractional ice coverage (in %) from 1973-2010. Also shown are the overall linear trends in 5% ice-on and ice-off dates (dashed lines), split linear trends for the years 1973-1997 and 1998-2010 (dotted lines), and means for years 1973-1997 and 1998-2010 (red lines). (b) As in (a), but for IFD. None of the split linear trends are statistically significant.

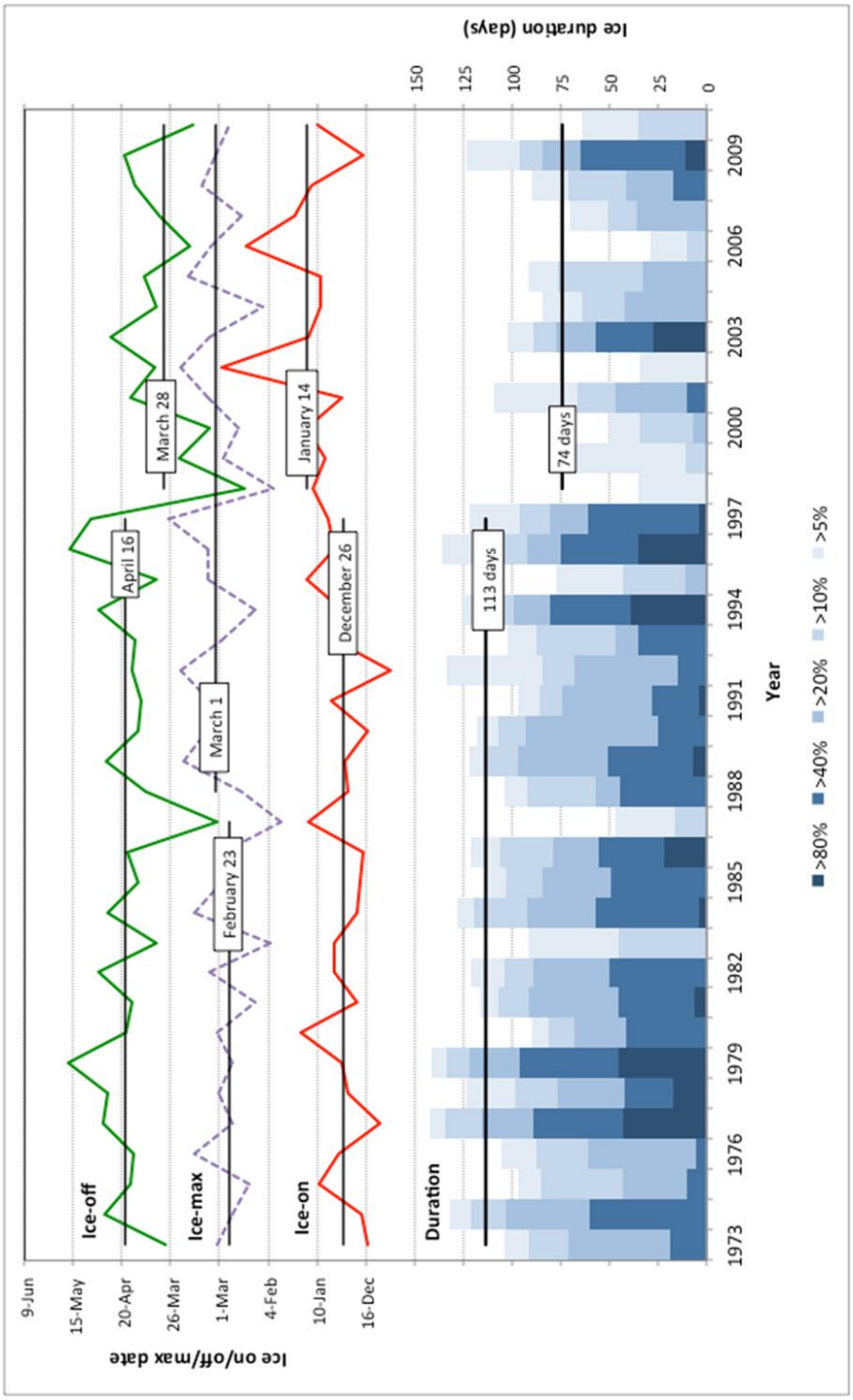

Figure 4: Lake Superior 5% ice-on and ice-off dates (solid lines), date of ice maximum (dashed line), and ice duration (bars, shaded by % coverage) from 1973-2010. Also shown are the mean values before and after the most statistically significant step change (i.e., 1998; except for 1988 in the case of ice-max; Table 1).

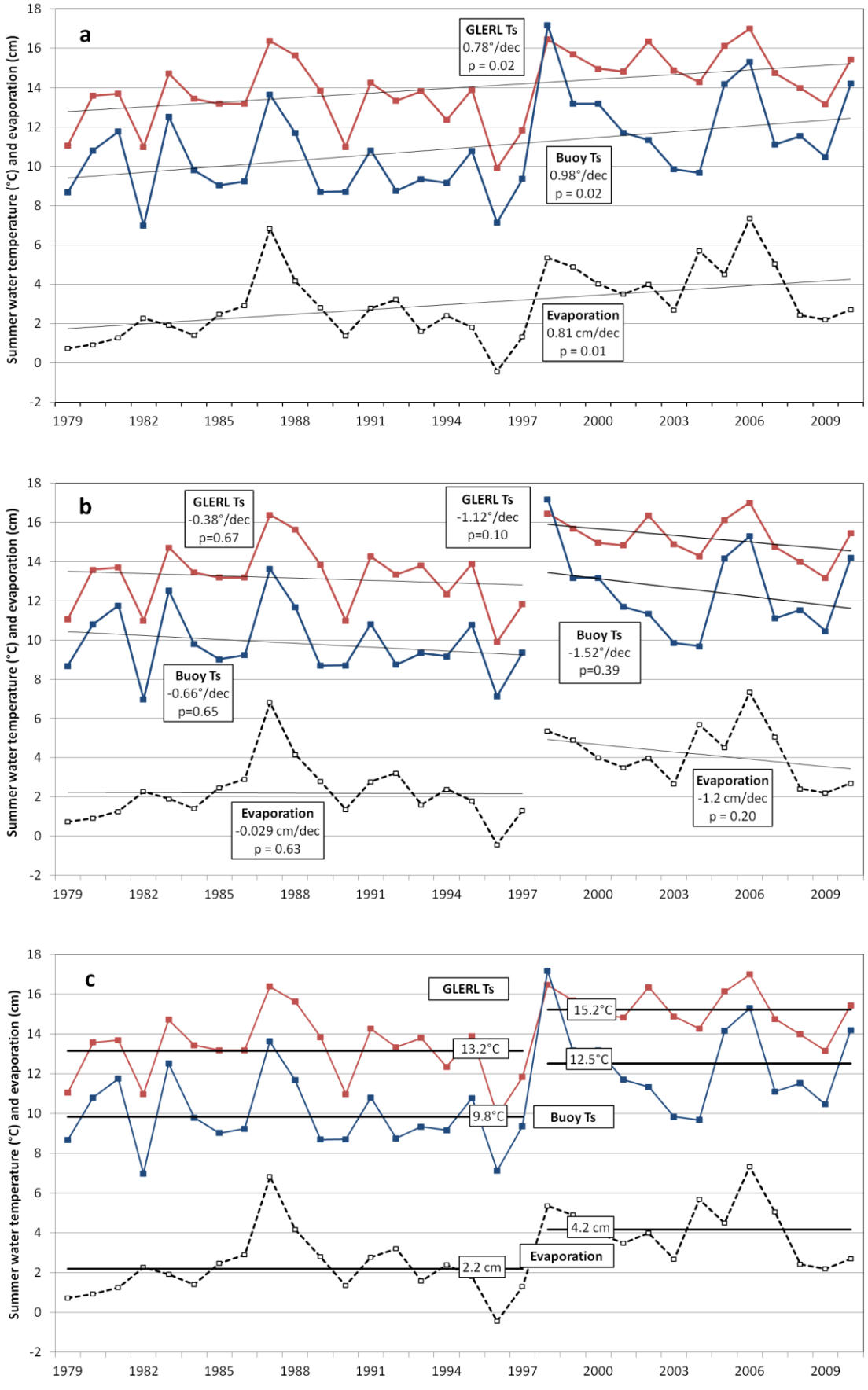
a
GLERL Ts
0.78°/dec
p = 0.02
Buoy Ts
0.98°/dec
p = 0.02
Evaporation
0.81 cm/dec
p = 0.01
b
GLERL Ts
-0.38°/dec
p=0.67
GLERL Ts
-1.12°/dec
p=0.10
Buoy Ts
-0.66°/dec
p=0.65
Buoy Ts
-1.52°/dec
p=0.39
Evaporation
-0.029 cm/dec
p = 0.63
Evaporation
-1.2 cm/dec
p = 0.20
c
GLERL Ts
15.2°C
13.2°C
12.5°C
9.8°C
Buoy Ts
4.2 cm
2.2 cm
Evaporation
Summer water temperature (°C) and evaporation (cm)
18
16
14
12
10
8
6
4
2
0
-2
1979
1982
1985
1988
1991
1994
1997
2000
2003
2006
2009

Figure 5: Lake Superior July, August, September (JAS) surface water temperature (T_s) and July, August (JA) total evaporation for the period 1979-2010. Also shown are the (a) overall linear trends, (b) split linear trends for the years 1979-1997 and 1998-2010, and (c) long-term means for 1979-1997 and 1998-2010. Statistical significance of the step changes in (c) are listed in Table 1.

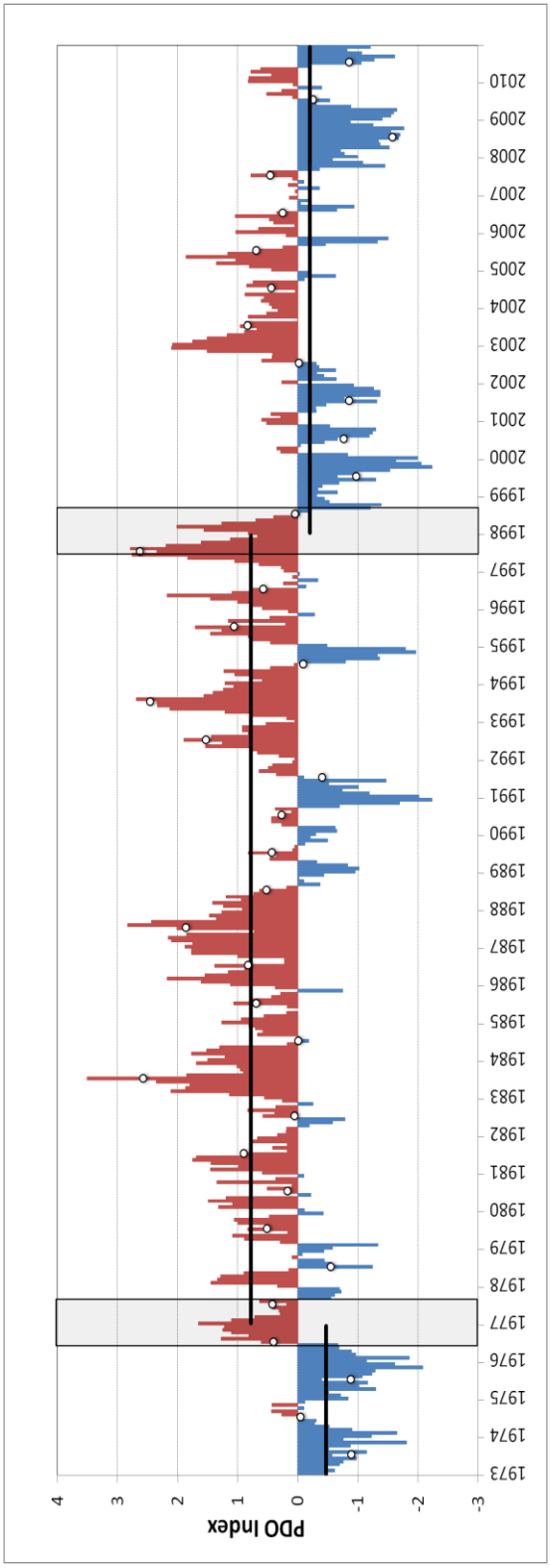

Figure 6: Monthly PDO index for the period 1973-2010. Dots indicate the summer PDO index (PDOs) for each year, with step changes occurring in 1977 and 1998. Solid black lines indicate long-term means of the PDOs for the period 1944-1976, 1977-1997, and 1998-2010.

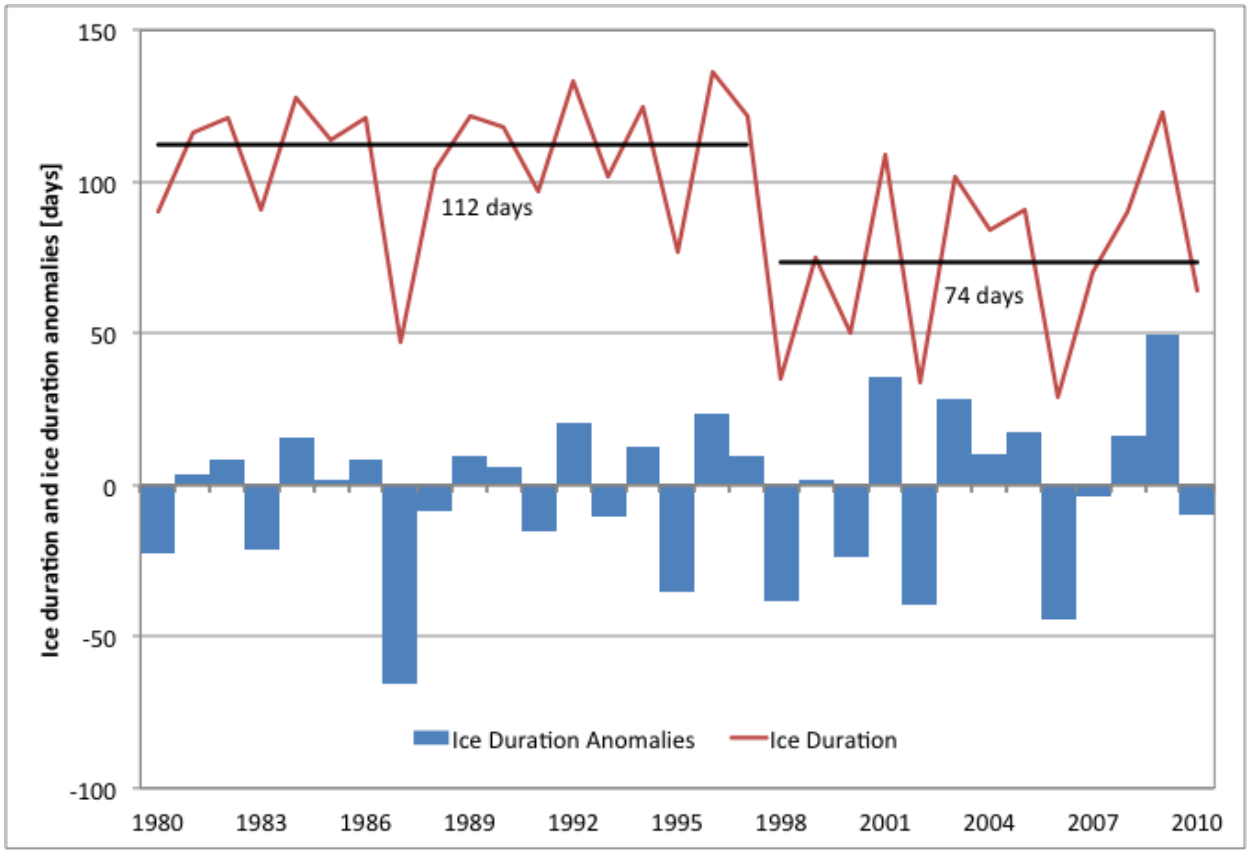

Figure 7: Ice duration (red line) and ice duration anomalies (blue bars) for 1980-2010. Means for the period 1979-1997 and 1998-2010 are shown (black lines).

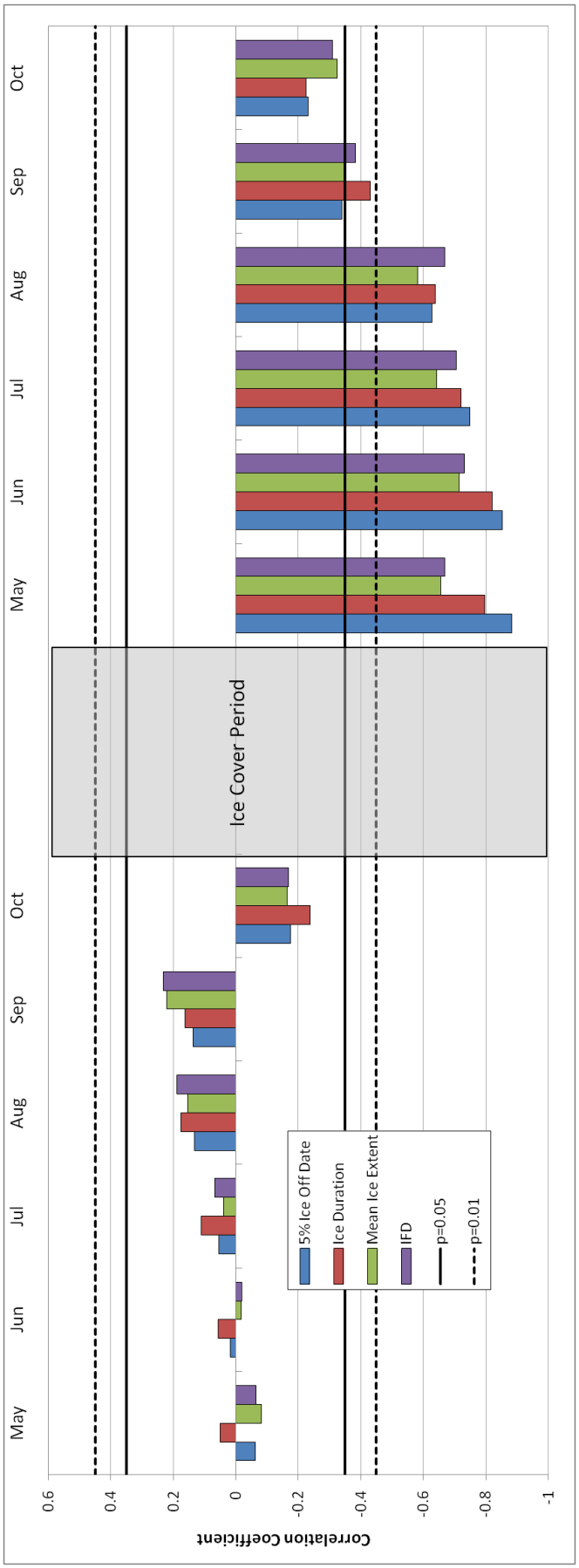

Figure 8: Correlation analysis: Monthly water temperature (GLERL) and ice cover metrics (5% ice off date, duration, mean extent, IFD). Solid black lines are p=0.05 significance level.

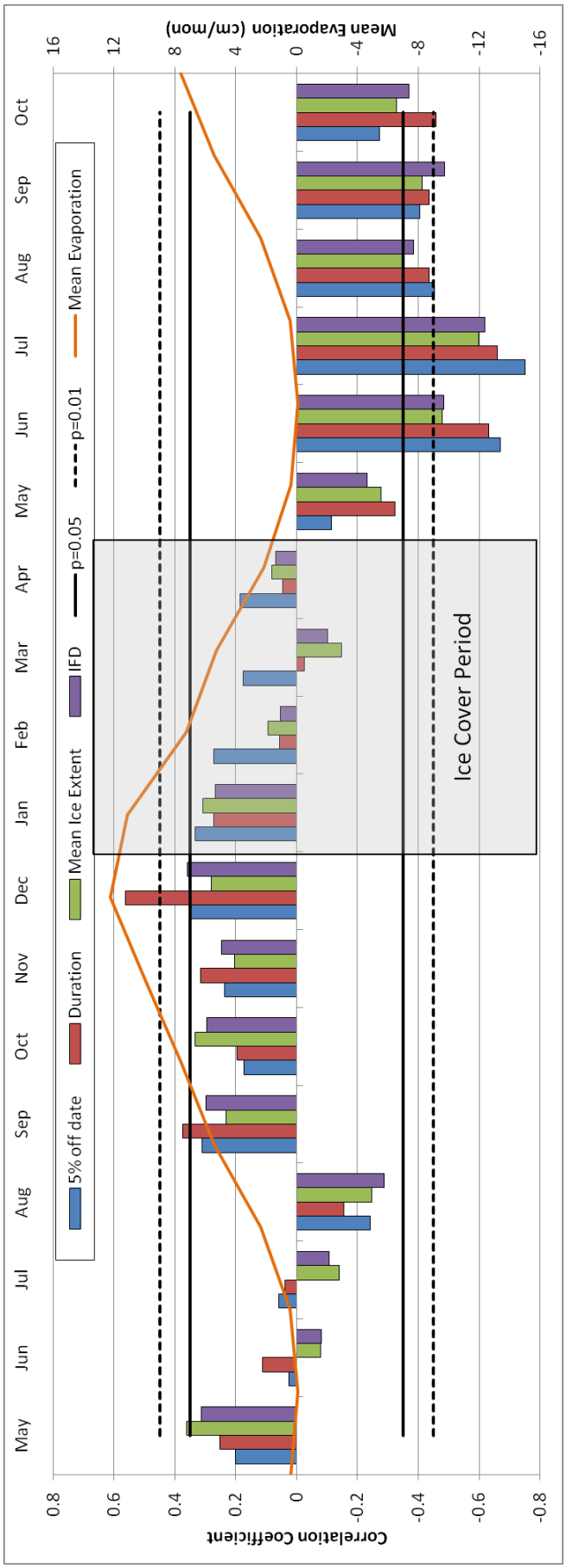

Figure 9: Correlation analysis: Monthly evaporation and ice cover metrics (5% ice off date, duration, mean extent, IFD). Solid black lines are p=0.05 significance level.

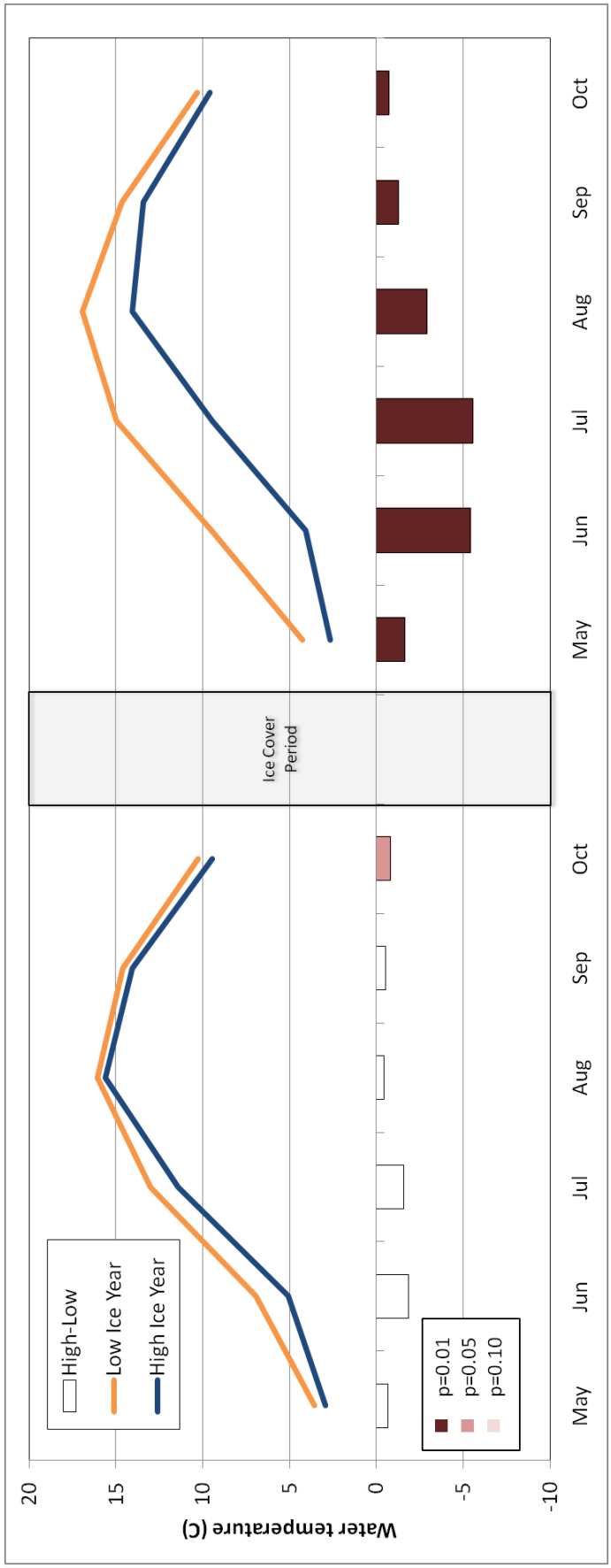

Figure 10. Composite analysis: Monthly absolute water temperature based on Table 2. Differences (high ice year – low ice year) are shown, with significance indicated by bar color.

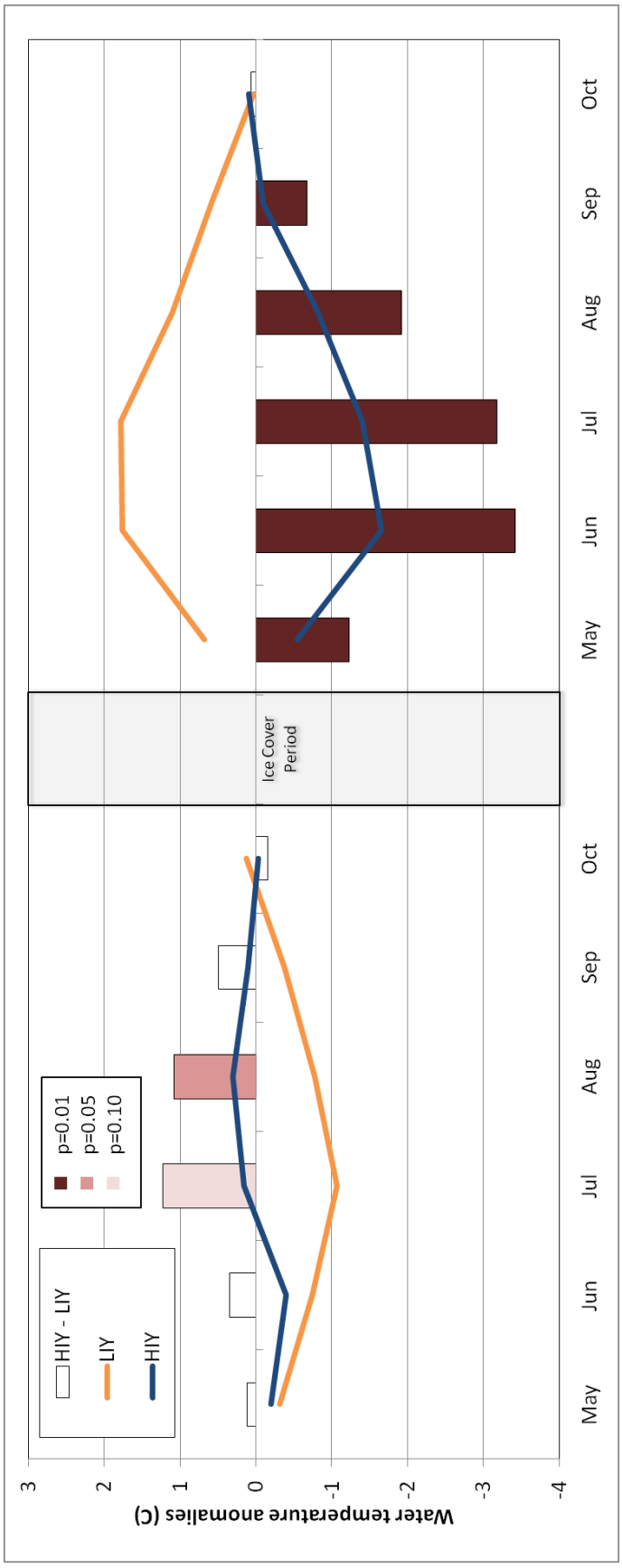

Figure 11: Composite analysis: Monthly water temperature anomalies based on Table 3. Differences (high ice year-low ice year) are shown, with significance indicated by bar color.

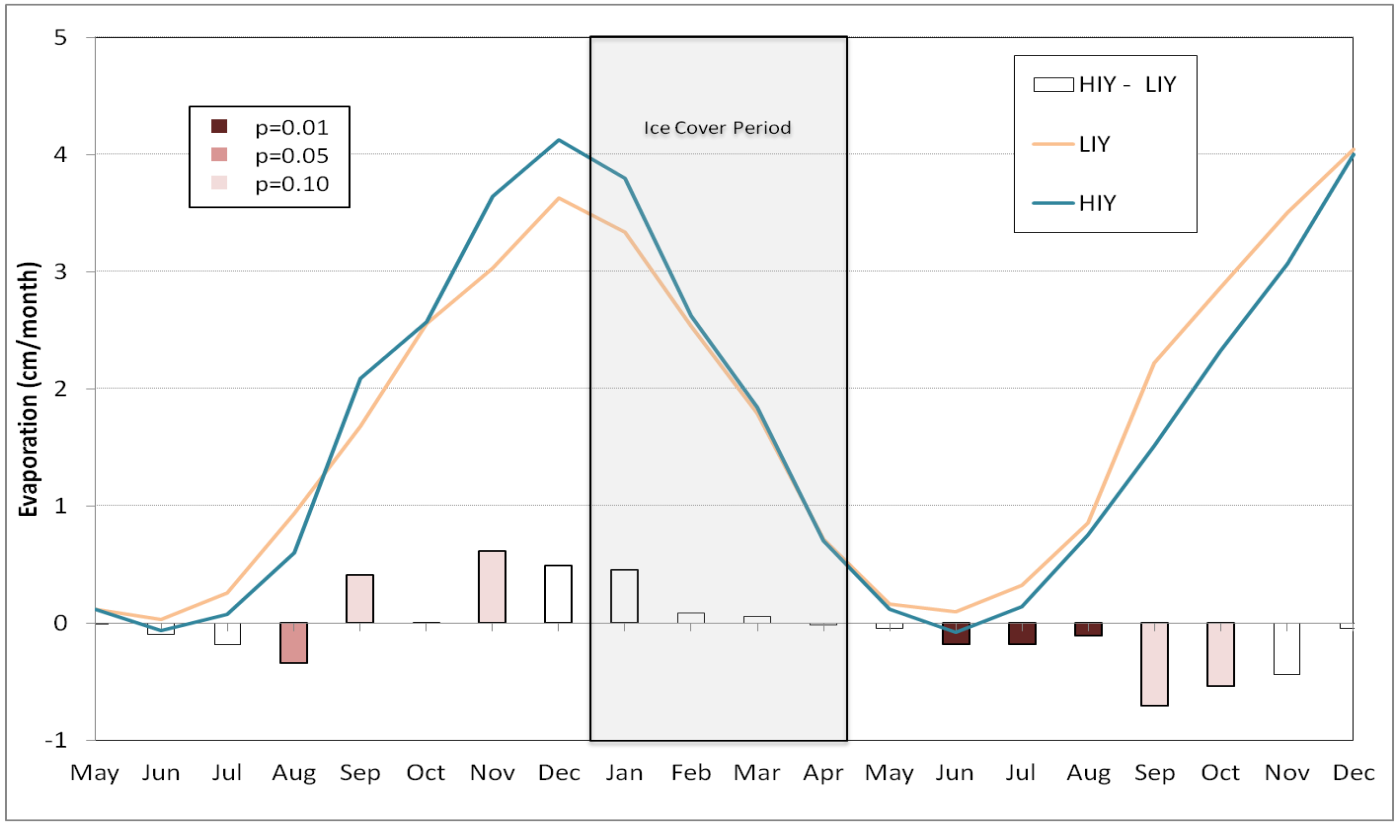

Figure 12: Composite analysis: Monthly absolute evaporation based on Table 2. Differences (high ice year-low ice year) are shown, with significance indicated by bar color. White bars are not significant.

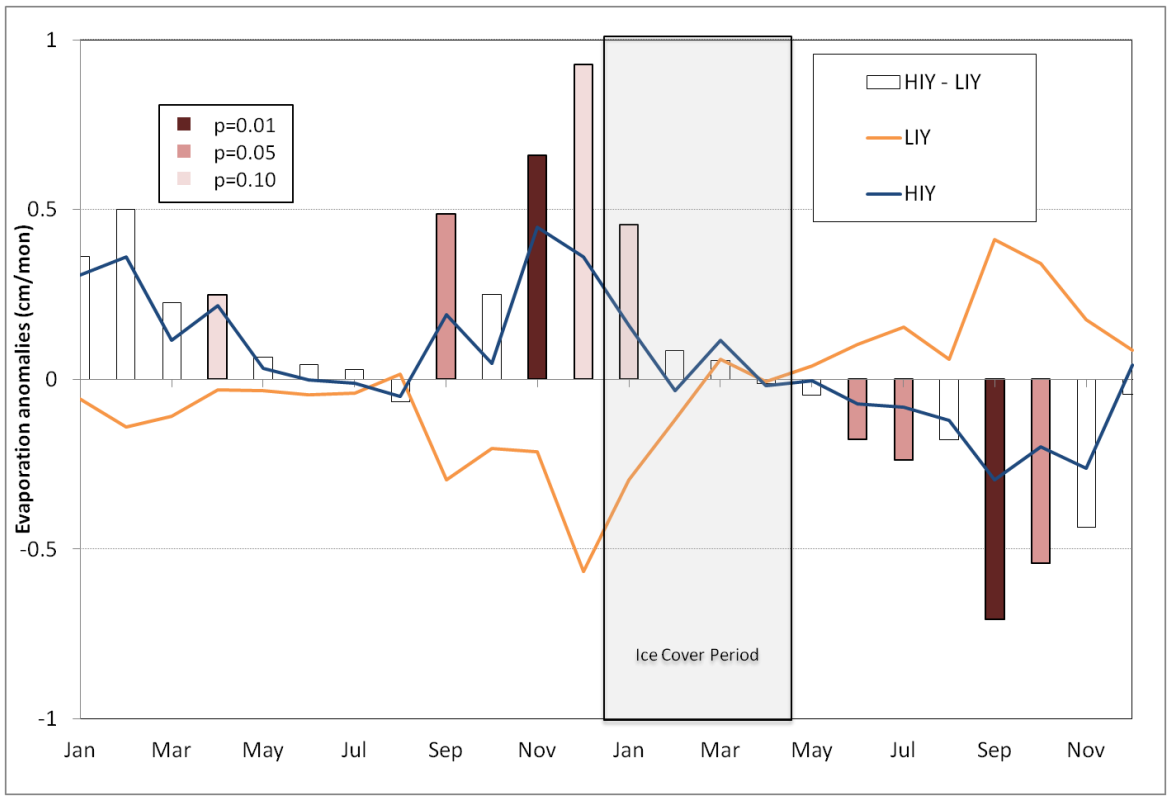

Figure 13: Composite analysis: Monthly evaporation anomalies based on Table 3. Differences (high ice year-low ice year) are shown, with significance indicated by bar color. White bars are not significant.

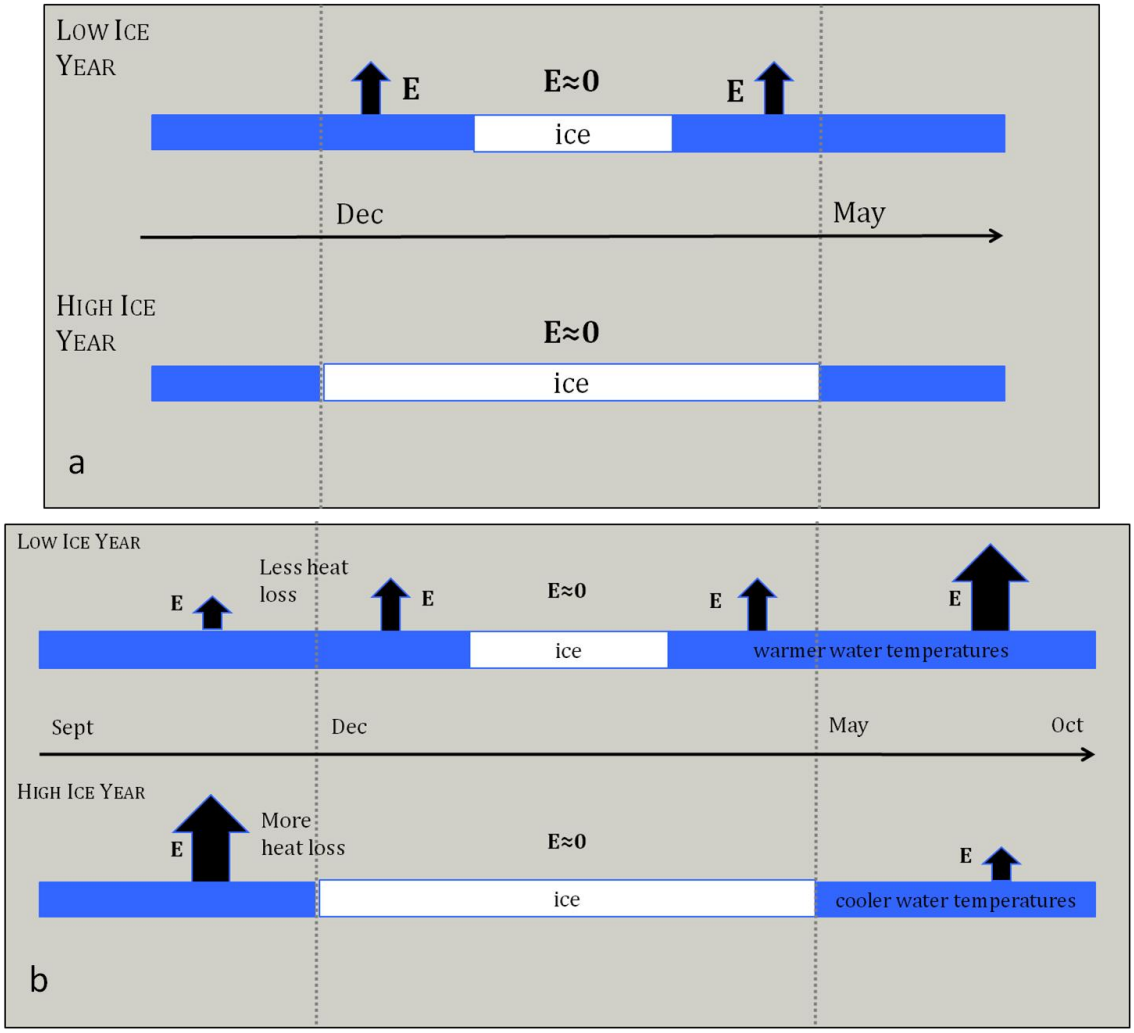

Figure 14: Schematic of interactions among water temperature, ice cover, and evaporation based on the "standard paradigm" (a) and results of the correlation and composite analysis (b).

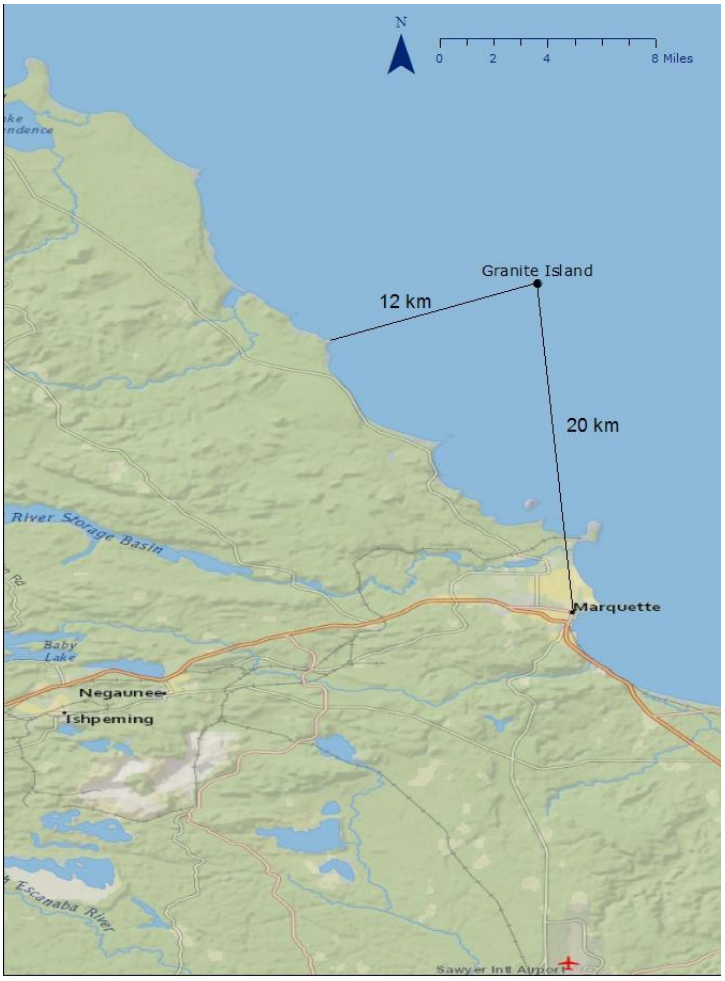

Figure 15: Location of meteorological station on Granite Island, Michigan. The station is 20 km from Marquette Harbor and 12 km from the nearest land.

Figure 16: Granite Island flux measurement instrumentation. The LI-7500, CSAT3, and KH2O krypton hygrometer are visible in the upper right-hand corner. Additional meteorological instruments measure wind speed and direction, rainfall, barometric pressure, air temperature, humidity, and water temperature (through an infrared thermometer) (photo c/o John Lenters).

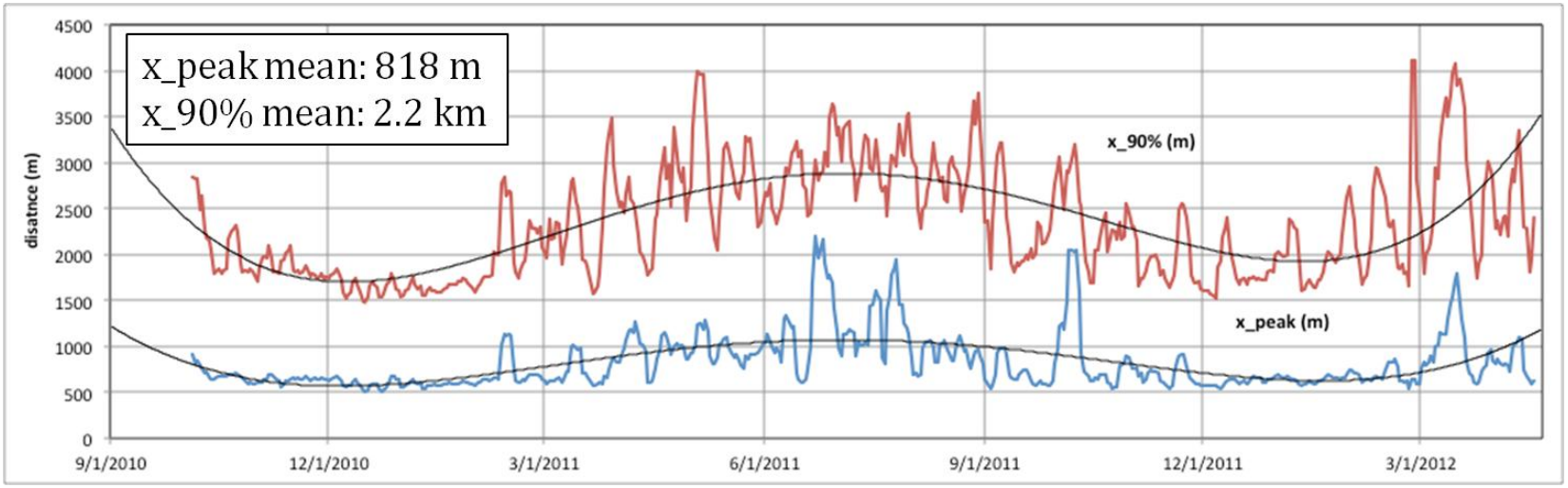

Figure 17: 7-day average flux footprint for Granite Island, MI. Both peak footprint distance (black line) and 90% footprint distance (grey line) are shown. Polynomial fits are for visualization of changes in footprint distance between seasons.

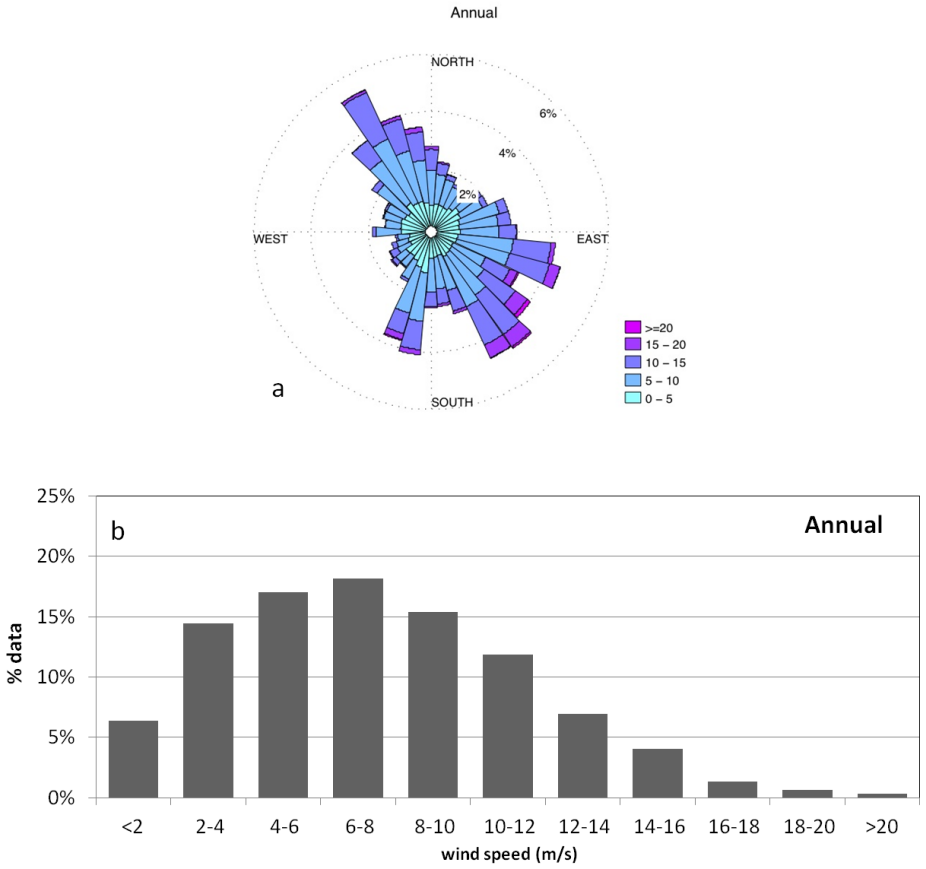

Figure 18: Half-hour wind speed and direction on Granite Island (Oct 6, 2010 – Apr 25, 2012) shown as a (a) wind rose diagram and (b) histogram of wind speeds.

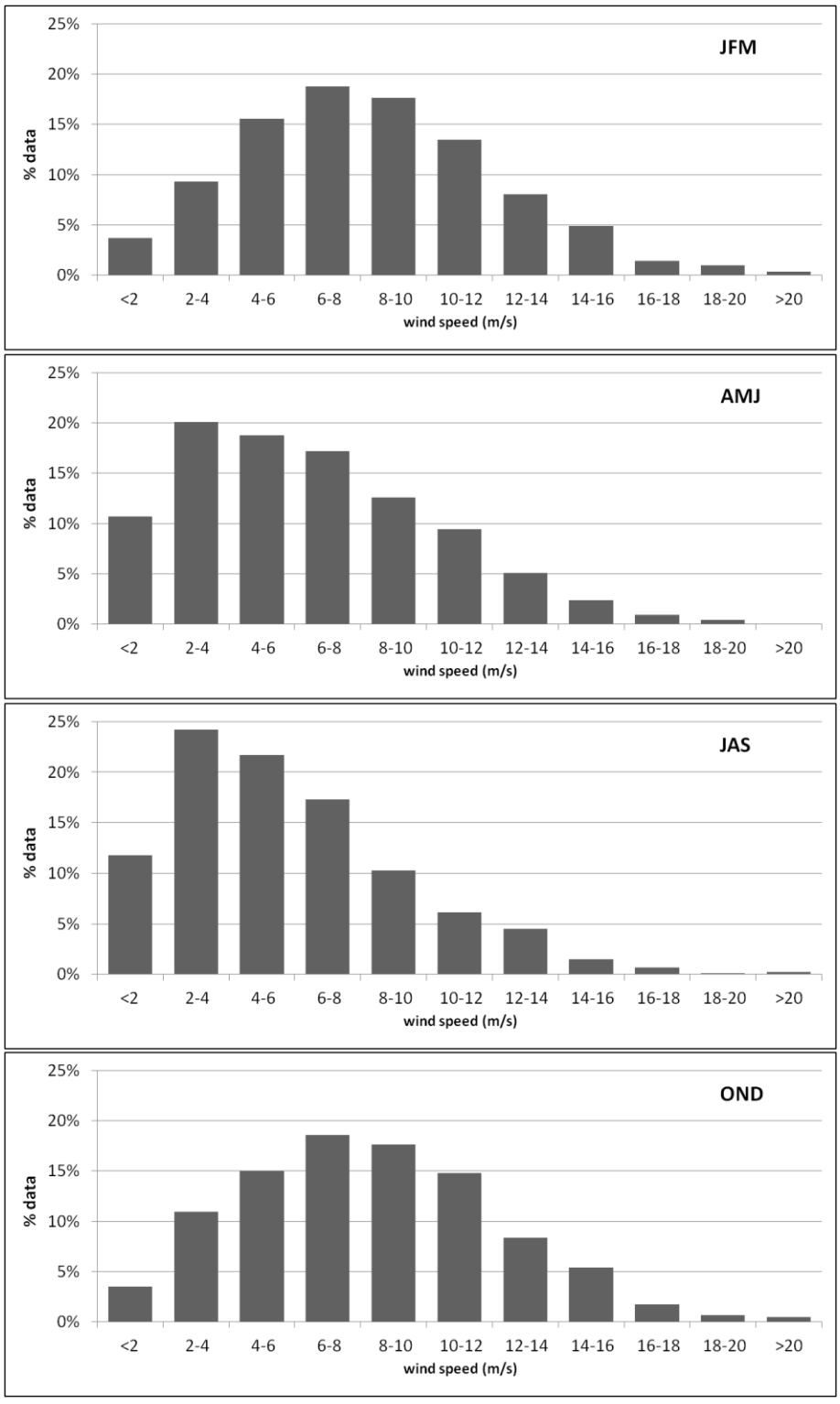

Figure 19: Half-hour average wind speeds by season (JFM, AMJ, JAS, OND) at Granite Island for the period October 6, 2010 – April 25, 2012. Y-axis shows the percentage of data.

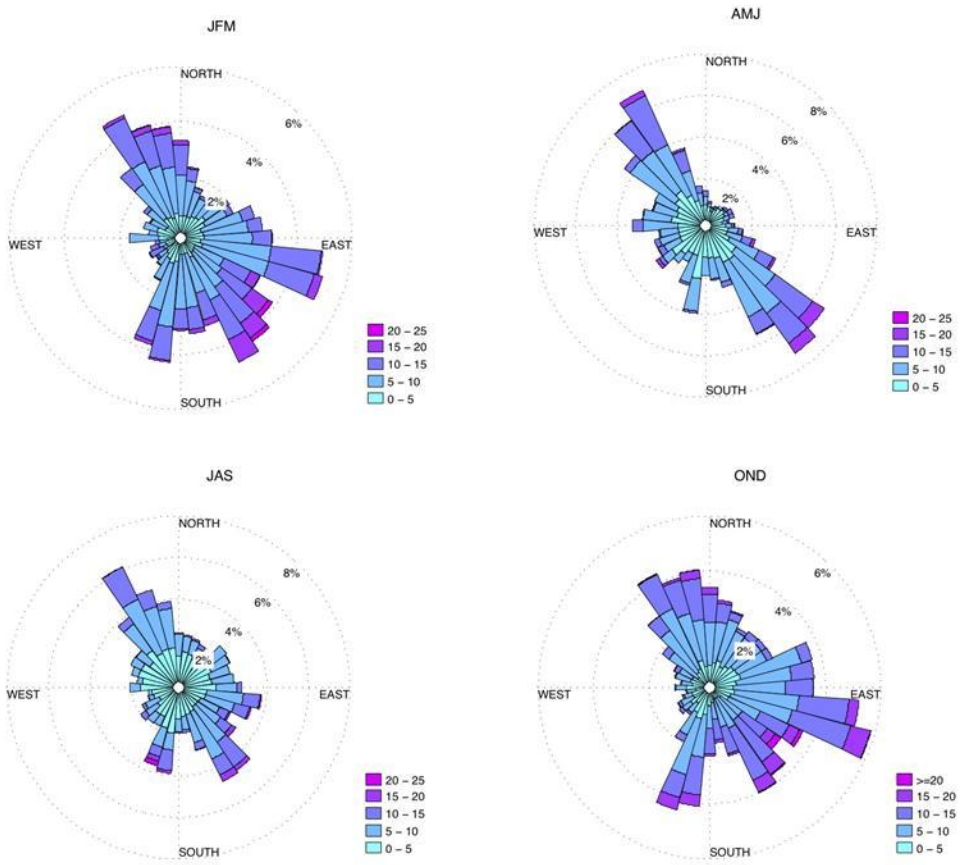

Figure 20: Seasonal (JFM, AMJ, JAS, OND) wind roses for Granite Island. Wind speeds listed are in m/s. Data is half-hour average wind speeds and directions.

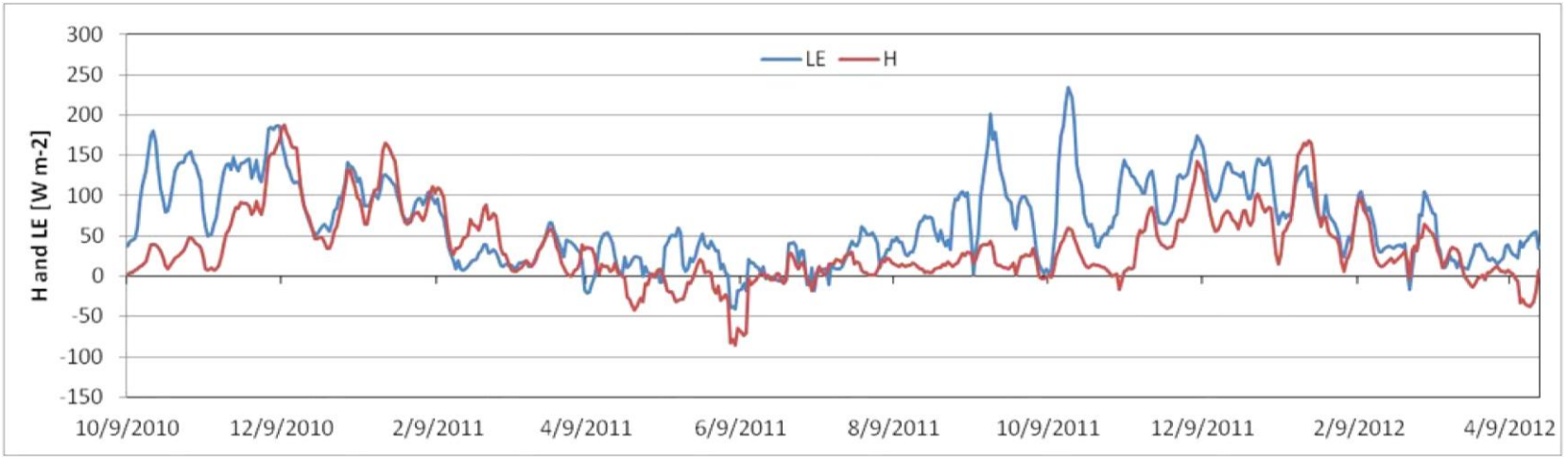

Figure 21: 7-day running means of sensible (H, red) and latent (LE, blue) heat flux at Granite Island from October 6th, 2010 – April 23, 2012.

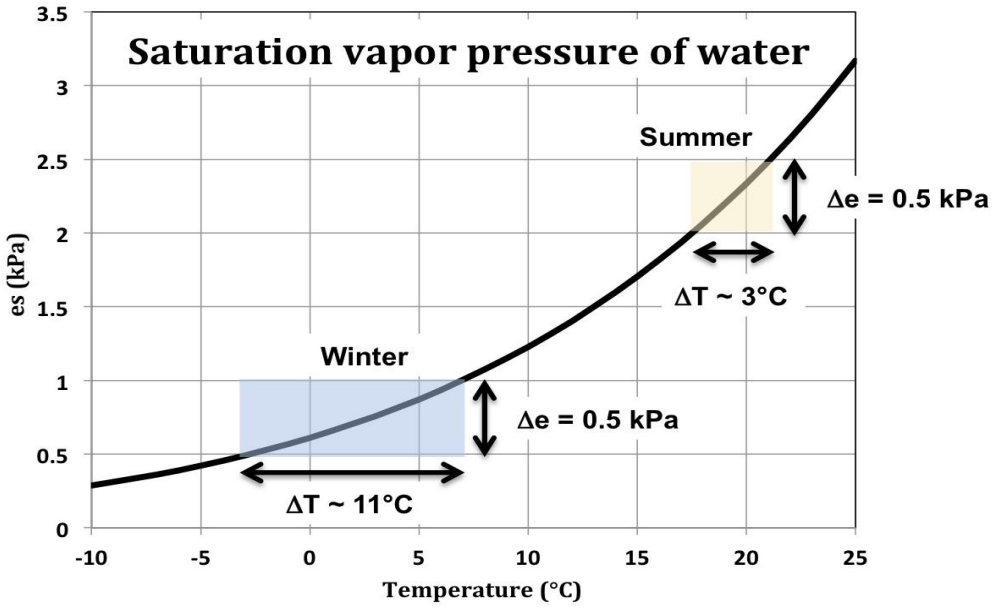

Figure 22: Saturation vapor pressure curve for water showing increased difference in temperature vs. vapor pressure at lower air temperatures. This results in larger amounts of sensible heat flux later in the winter season as compared to latent heat flux.

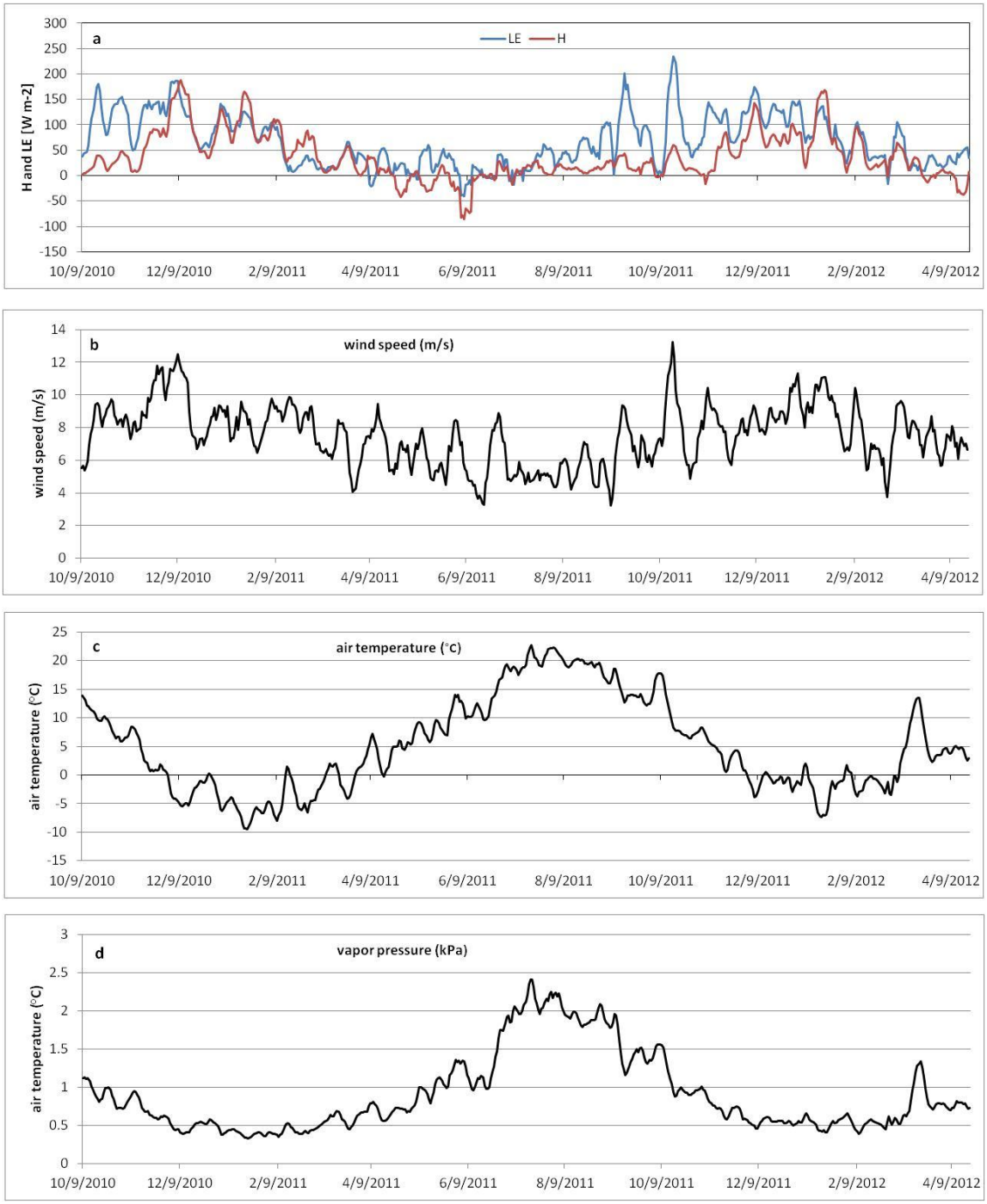

Figure 23: 7-day averages of (a) latent and sensible heat flux, (b) wind speed, (c) air temperature, and (d) vapor pressure for the period October 9, 2010 – April 20 2011.

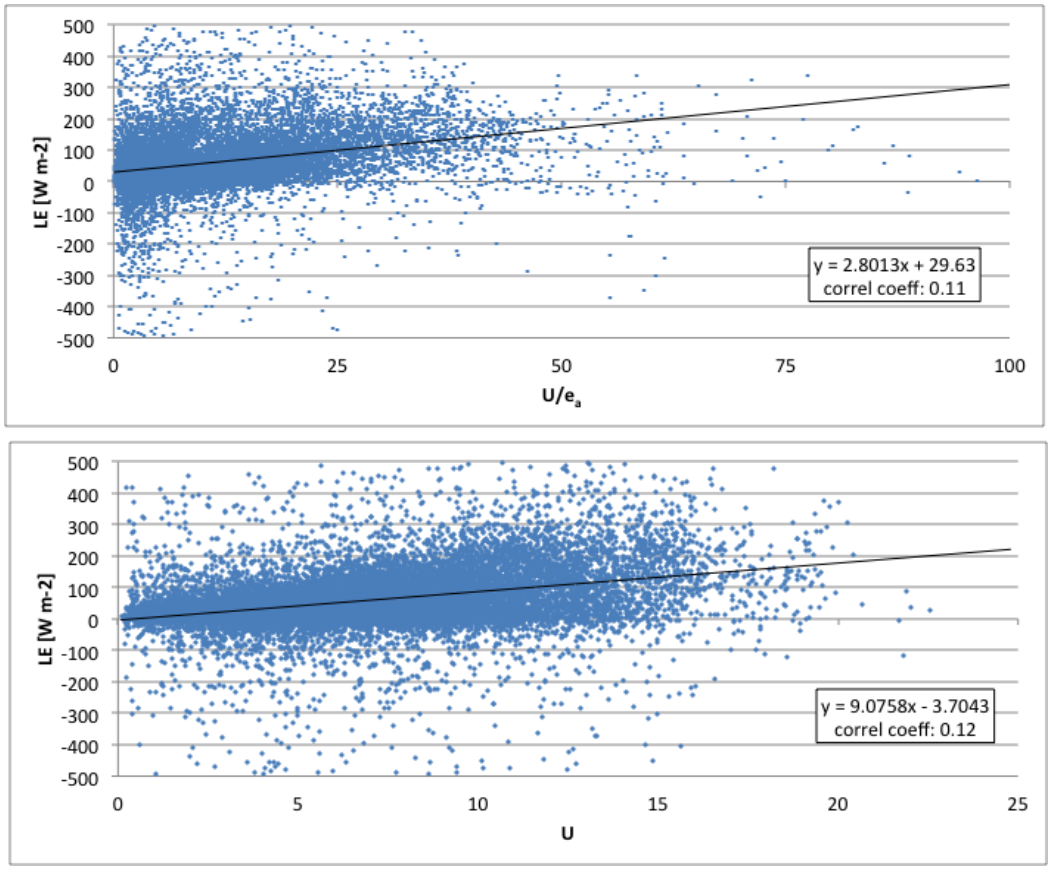

Figure 24: Linear regression of LE vs. U/e_a, using daily average values. Regression equation is displayed in box in upper right hand corner.

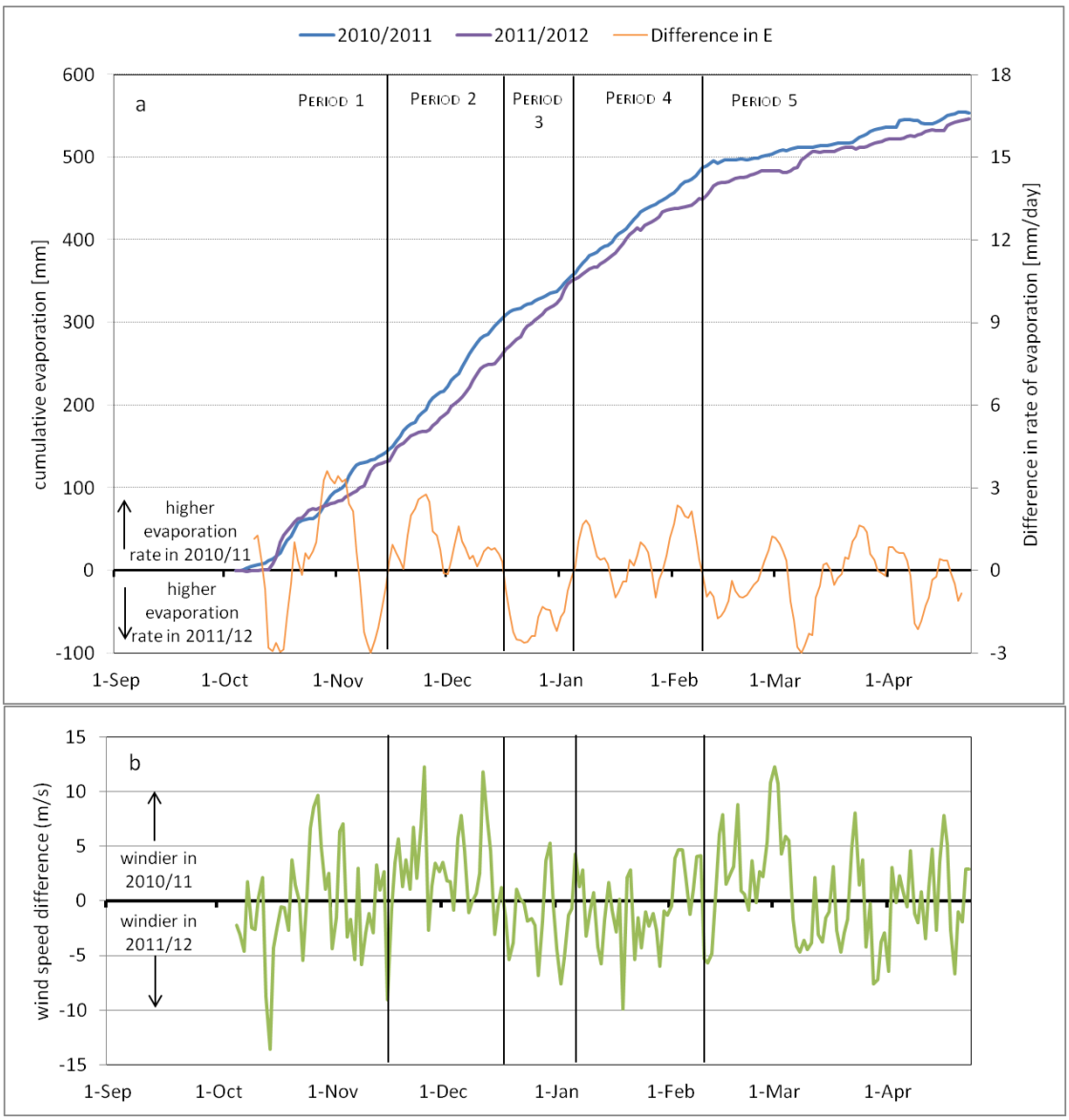

Figure 25: (a) Winter season cumulative evaporation and evaporation difference (2010/11 minus 2011/12), split into five periods based on differences in rates of evaporation between the two years. Period 1: October 6 – November 15, Period 2: November 16- December 16, Period 3: December 17 – January 3, Period 4: January 3 – February 10, Period 5: February 10 – April 23. (b) Difference in wind speeds between 2010/11 and 2011/12.

Figure 26: Map showing the location of Granite Island and Stannard Rock. The distance between the two sites is 55 km. White circles show the 8-km radius for which average water depth was calculated at each station.

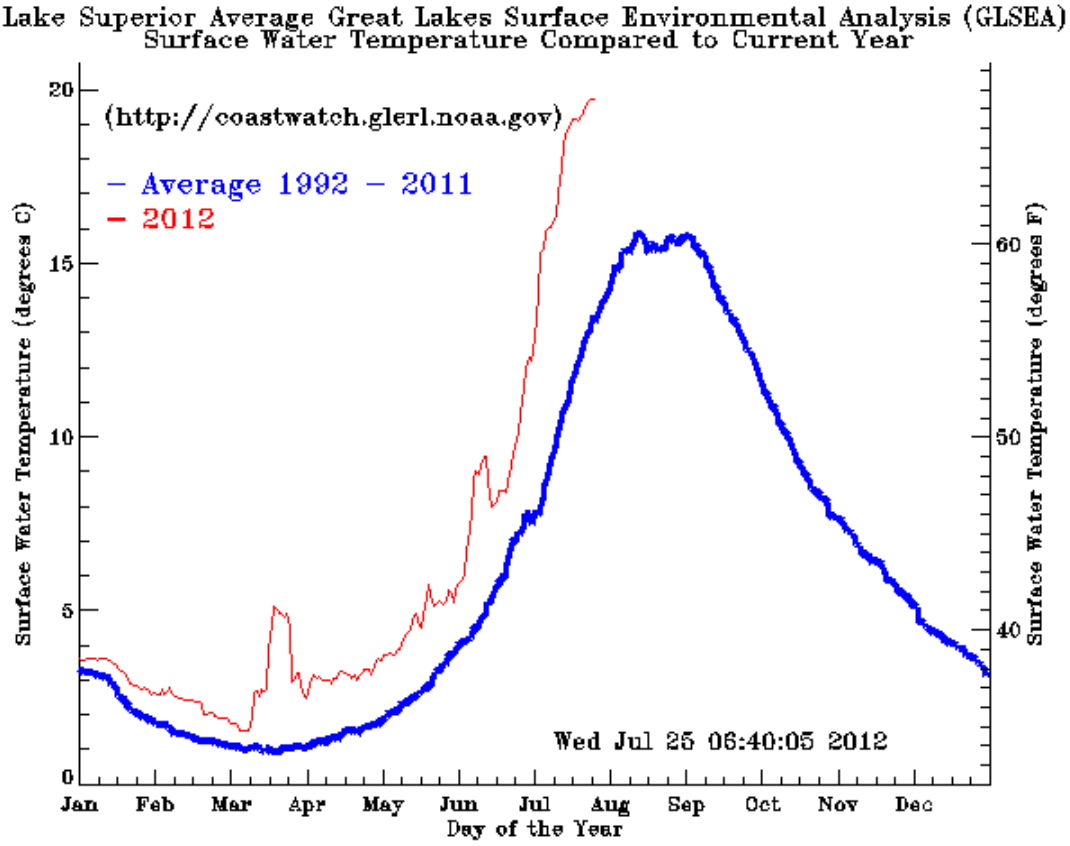

Figure 27: Lake-wide average surface water temperature for Lake Superior during 2012 (red line) and the mean period 1992-2011 (blue line). Figure taken from the Great Lakes Surface Environmental Analysis (GLSEA) at GLERL: http://coastwatch.glerl.noaa.gov/statistic/gif/avgtemps-s_1992-2011.gif